Preparation of Polymer Nano Composites

A Thesis Submitted

in partial fulfillment of the requirements
for the degree of

Master of Technology

by

Thumati Jayasimha

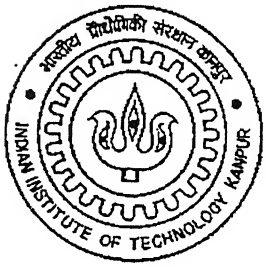

to the

DEPARTMENT OF CHEMICAL ENGINEERING
INDIAN INSTITUTE OF TECHNOLOGY, KANPUR

June, 2005

CERTIFICATE

It is certified that the work contained in the thesis entitled "**Preparation of Polymer Nano Composites**" has been carried out by **Thumati Jayasimha** under my supervision and that it has not been submitted elsewhere for a degree.

Dr. Anil Kumar
Professor,
Department of Chemical Engineering
Indian Institute of Technology
Kanpur-208016.

ACKNOWLEDGEMENTS

I feel pleasure in expressing my deep sense of gratitude towards my thesis supervisor Prof. Anil Kumar for his descending guidance, constant encouragement and valuable suggestions through out the course of this work. He has been very much encouraging at all times and has immense trust in our abilities. It has been most exciting phase of my career and it indeed gives me great pleasure and privilege to have worked with him. I learned a lot from, which would be of great help in future. Thank you, sir!

I would like to thank all the faculty members of Chemical Engineering Department, IIT Kanpur who helped me a lot during my course work and for their useful suggestions. My special thanks to my lab mates Mr. G. Pugazhenthi, Jhansi, Anisia ji, Sony ji, Sadhana ji, Kiranmai, sunder lal, Ram Pravesh, Manoj Kumar and Ajith Kumar with whom I worked during my thesis, for their help and valuable suggestions. Above all, they have been good friends and companions. I am also thankful to Diwakar ji for helping me during impact strength tesing, Sasi for helping in TGA analysis, Krishna Prasad for helping in TEM analysis, Sharmaji and Chhotu for their constant help; to all my class mates, who made my stay so comfortable at IITK.

My special thanks to my friend Babai, without his company I wouldn't have stayed here for 2 years. I would like to thank Ramana mava, Aswani mavayya, konda, Rajesh, Dinesh, Chinna, Anji, Ravi, M.V.P.K, Ramu, Sudheer, Current srinu, for the unforgettable moments, which I had with them during my stay at Hall 7. I express my hearty gratitude to my dear friend Veni for sharing all my sorrows and pleasures.

Finally, I express my profound gratitude and affection to my parents and sister, for their encouragement, understanding, patience and support.

June, 2005

Thumati Jayasimha

ABSTRACT

Polymer syrup of polymethylmethacrylate reinforced with 2% non settling nano alumina particles was prepared by dual initiating system containing Benzoylperoxide (BPO), Azobisisobutyro nitrile (AIBN) and Dimethylaniline (DMA). Nano alumina particles were prepared using Auto Ignition of aluminum nitrate and urea. The alumina surface was treated with a coupling agent, methacrylol isocyanate. The XRD analysis showed an average grain size of 28 nm for nano alumina particles and 38 nm for modified nano alumina particles. The polymer syrup prepared as earlier was applied between two PMMA sheets and Poly carbonate sheets of 2 mm thickness and 12 cms x 12 cms dimensions each and tested with Bullet Firing Machine and Drop Weight Impact Testing Machine. The results show that after firing with bullet speed of 62 m/s, the damaged area of PMMA composite sheet was 59% with syrup while that with non settling nano particles was 9% only. As opposed to this, Polycarbonate composite sheets prepared using polymer syrup fired with bullet speed of 91 m/s showed a damaged area of 34%, while that using polymer syrup with nano particles showed no damage. Drop Weight Machine results show an increase in maximum load of 3 times for PMMA sheets with polymer syrup with non settling nano particles inside, when compared with empty PMMA sheets, whereas an increase in maximum load of 2 times was observed for Polycarbonate sheets with polymer syrup containing non settling nano particles inside as compared to non joined Polycarbonate sheets.

Contents

List of Tables

List of Figures

Chapter 1

INTRODUCTION

1.1 Polymer nano composites:

Polymer nano composites are the materials having inorganic nano particles (with one dimension in the nanometer ($\sim 10^{-9}$m range) dispersed in polymer medium [1]. These have been of the recent interest and exhibit superior mechanical, electrical properties different from the original ones due to synergistic interactions between them [2, 3]. Usually polymers have lower strength compared to metals and ceramics. Earlier inorganic fillers having their dimensions in microns ($\sim 10^{-6}$m) has been proved to be an effective way for the improvement of the mechanical properties, particularly the toughness of the polymers. However, the filler contents needed for such improvements are as high as 20% by volume [4, 5]. This high filler content causes deterioration in the processing of the polymer and give rise to an increase in weight of the end products as compared to the polymers with out it. This limits various applications of these materials in the transportation sub segments, in the electrical and electronic industry, and in the appliance and equipment industry. The basic advantages of polymers as material, their ease of processing and light weight, get therefore lost.

In view of the above, a composite with improved properties and lower particle concentrations is highly desired. An attempt to overcome this problem was to reinforce polymers with fillers, which were in nanometer range. The unique feature of nano fillers is their extremely high surface area and for a well dispersed system, even low filler volume fractions (1-2%) provide large interfacial area through which the bulk properties of the polymer can be altered [6]. The mechanical properties of the composites filled with

micron sized filler particles are inferior to those filled with nano particles of the same filler [7]. The physical properties, such as surface smoothness and barrier properties cannot be achieved by using micron sized particles. The embedding of inclusions in the host matrix to make composites gives material properties different from either phase alone. Using this approach, polymer properties can be improved while maintaining their light weight and ductile nature [8,9].

In general there are two types of brittle fracture. The first type of fracture being transgranular in nature. In this, the fracture travels inside the grain of the material and changes direction depending upon the orientation of atoms in each grain (see fig 1.1). This type of fracture occurs in materials in which the phase in the grains is weak compared to that in grain boundaries i.e., when the crack reaches a new grain, it chooses the path of least resistance.

The second type of fracture is intergranular fracture in which the crack travels along the grain boundaries and not through the actual grains (see fig 1.2). This type of fracture usually occurs when the phase in the grain boundary is weak and brittle (for example Cementite in iron's grain boundaries).

In the matrix grains, with nano particles the later can make the main cracks to deflect, so the paths for the crack propagation are very tortuous and are impeded in many places, resulting in higher fracture energy, this way enhancing its toughness [10]. The effects of filler on the mechanical and other properties of the composites depend strongly on its shape, particle size, aggregate size, surface characteristics and the degree of dispersion [11]. The nature of the filler/matrix interface also dictates the properties of the composites. Hence the preparation of the nano particles is of great importance. The

critical factor in the synthesis of nano particles is to make sure that there is no agglomeration of the particles and the particle should be in crystalline in nature.

1.2 Different Techniques for Nano Particle Preparation:

In general there are many types of nano particles like inorganic oxide particles such as alumina, silica and metal particles such as silver, copper. Nano particles were generally synthesized by Coprecipitaion, Sol gel processing, Micro emulsions, Hydrothermal/Solvothermal [12].

1.2.1 Coprecipitation:

Coprecipitation is the earliest technique for the preparation of nano particles [13]. In this technique the nano particles are synthesized by the coprecipitation of sparingly soluble products from aqueous solutions followed by the thermal decomposition of those products to oxides. Coprecipitaion reactions involve the simultaneous occurrence of nucleation, growth, coarsening, and/or agglomeration processes [14]. Coprecipitation reactions tend to exhibit the following characteristics [15].

(i) The products of the precipitation reactions are generally sparingly soluble species formed under conditions of high super saturation.

(ii) Such conditions dictate that nucleation will be a key step of the precipitation processes and that a large number of small particles will be formed.

(iii) Secondary processes, such as Ostwald ripening and aggregation, will dramatically affect the size, morphology, and properties of the products.

(iv) The super saturation conditions necessary to induce precipitation are usually the result of a chemical reaction.

Generally, chemical reactions are chosen such that it result in products with low solubilities, and the solution quickly reaches a super saturated level [16, 17].

Su et al. [18] used this technique for the preparation of $Y_3Al_5O_{12}$ (YAG-Yitrium Aluminum Garnet). The YAG precursor was prepared by using Y_2O_3, $Al(NO_3)_3.9H_2O$ as starting materials. The $Y(NO_3)_3$ solution was prepared by dissolving Y_2O_3 in dilute HNO_3. Aqueous solutions of $Y(NO_3)_3$ and $Al(NO_3)_3$ were mixed with Ammonia as the precipitator. The mixed nitrate solution was added drop-wise into the precipitant solution under vigorous stirring. The precipitate was then separated and washed with deionized water. After washing, the precipitate was dried and ground and sintered at various temperatures.

Chen et al. [19] prepared strontium ferrite nano particles using coprecipitation technique. Polyacrylic acid sodium salt with an average molecular weight of 2100 was used as the protective agent. To prepare strontium ferrite nano particles, a PAA aqueous solution (2.34 M) was first prepared by directly adding the desired amount of PAA to water and adjusting its final pH value to 1.8 with 0.1N HNO_3. Then the PAA aqueous solution was mixed with an equal volume of aqueous solution containing strontium nitrate (0.01 M) and ferric nitrate (0.008 M). Compared with the total concentration of Sr^{2+} and Fe^{3+} ions, the concentration of PAA used was recognized to be high enough as a protective agent. To ensure complete precipitation of Sr^{2+} and Fe^{3+} ions, high concentrations of NaOH (2N) was added to the mixed solution under stirring to yield the mixed hydroxide precipitates. The pH value of final solution was 13.8. After being centrifuged at 15000 rpm for 10 min, the mixed hydroxide

precipitates were washed two times with 225 ml water to remove sodium and nitrate ions and then vacuum dried at 70^0C.

1.2.2 Sol-Gel Processing:

Sol-gel processing refers to the hydrolysis and condensation of alkoxide-based precursors such as Si $(OEt)_4$ (tetraethyl orthosilicate, or TEOS) [20]. The sol-gel process can be characterized by a series of distinct steps [21-23].

Step 1: Formation of different stable solutions of the alkoxide or solvated metal precursor (the sol).

Step 2: Gelation resulting from the formation of an oxide- or alcohol- bridged network (the gel) by a polycondensation or polyesterification reaction that results in a dramatic increase in the viscosity of the solution.

Step 3: Aging of the gel (syneresis), during which the polycondensation reactions continue until the gel transforms into a solid mass, accompanied by contraction of the gel network and expulsion of solvent from the gel pores. Ostwald ripening (also referred to as coarsening, is the phenomenon by which smaller particles are consumed by larger particles during the growth process) and phase transformations may occur concurrently with syneresis. The aging process of gels can exceed 7 days and is critical to the prevention of cracks in gels that have been cast.

Step 4: Drying of the gel, when water and other volatile liquids are removed from the gel network. This process is complicated due to fundamental changes in the structure of the gel. The drying process has itself been broken into four distinct steps:

(i) the constant rate period, (ii) the critical point, (iii) the falling rate period,

(iv) the second falling rate period.

If isolated by thermal evaporation, the resulting monolith is termed a *xerogel.* If the solvent (such as water) is extracted under supercritical or near super critical conditions, the product is an *aerogel.*

Step 5: Dehydration, during which surface- bound M-OH groups are removed, thereby stabilizing the gel against rehydration. This is normally achieved by calcining the monolith at temperatures up to 800^0C.

Step 6: Densification and decomposition of the gels at high temperatures (T>800^0C). The pores of the gel network are collapsed, and remaining organic species are volatilized.

Shen et al. [24] prepared nano particles of $Li_4Ti_5O_{12}$ using sol-gel technique. Tetra butyl titanate [Ti $(OC_4H_9)_4$] and isopropyl alcohol were first mixed with mole ratio of 1:60 (A solution). Lithium acetate was dissolved into the mixture solutions of isopropyl alcohol/ deionize water/ acetate acid (B solution). With vigorous stirring, B solution was gradually dropped into A solution and then a clear solution was produced. After aging for 3 h, a milk white gel formed. The resulting gelatin was heated at 80^0 C to extract our excess isopropyl alcohol and yield an organic precursor. Fine white powders were obtained by calcining the precursors in air at various temperatures (400-800^0 C) for 4 h.

Want et al. [25] used sol-gel technique for the preparation of aluminum borate nano wires. High purity $Al(NO_3)_3$ and H_3BO_3 in mol ratio 1:3, 1:4, and 1:6 were mixed together in deionized water. Citric acid was added to serve as ferment. The mixture solution was evaporated at 150^0C in an oven for 10h. Then the gel was got. The above gels were put in crucibles, respectively. The crucibles were heated in a muffle at 750^0C for 4 h under ambient atmosphere. The gel resultant of the solution of $Al(NO_3)_3$ and

H_3BO_3 in mol ratio of 1:3 was also heated at 1050^0C for 4 h. after heating, white powders were obtained. All solid powders centrifuged in distilled water to remove the impurities possibly remaining in the final products, and finally dried at 60^0C in air.

Mao et al. [26] prepared nano crystals of Anatase TiO_2 using sol-gel technique with acrylic acid as surface modifier. 1 ml tetra butyl titanate (TBT) AND 0.8 ml acrylic acid were added into 8.2 ml ethanol. The mixture was held to react at room temperature (18^0C) for 10 min and slowly dropped into a hot solution (pH=1) of 1 ml nitric acid and 39 ml distilled water at 70^0C, to allow the hydrolysis reaction at 70^0C for 3 h. then the pH value of the solution was adjusted to 7 using 5 M ammonia solution, which resulted in the deposit of nano-TiO_2 sol particles from the liquid phase. The deposit was separated from the solution, dried under infrared heat lamp (80^0C), and illuminated under a 250 W mercury vapor lamp for 8h. The temperature of the sample was about 64^0C during the UV treatment.

1.2.3 Hydrothermal/Solvothermal Processing:

In a sealed vessel (bomb, autoclave, etc.), solvents can be brought to temperatures well above their boiling points by the increase in autogenous pressures resulting from heating. Performing a chemical reaction under such conditions is referred to as solvothermal processing or, in the case of water as solvent, hydrothermal processing [27].

The critical point for water lies at 374^0C and 218 atm. and for temperatures and pressures above these, water is said to be supercritical state. Supercritical fluids in general exhibit characteristics of both a liquid and a gas: the interfaces of solids and supercritical fluids lack surface tension, yet exhibit high viscosities and easily dissolve chemical compounds that would otherwise exhibit low solubilities under ambient

conditions [28]. Solvothermal processing allows many inorganic materials to be prepared at temperatures substantially below those required for traditional solid-state reactions. Unlike the cases of coprecipitation and sol-gel methods, which also allow for substantially reduced reaction temperatures, the products of solvothermal reactions are usually crystalline and do not require post annealing treatments[29].

Yang et al. [30] used this techniques for the preparation of nano particles of transition metal Diselenides MSe_2 (M= Ni, Co, Fe). Elemental Se(~3.75 mmol) and powdered NaOH(~7.5 mmol) were put into a 50ml conical flask that already had contained 25ml of solvent such as distilled H_2O, N,N-dimethyl formaldehyde (DMF), pyridine (Py), acetyl acetone (acac), and ethylenediamine (en). A small amount of hydrazine (~0.14 mL) was added into the solution under violent stirring. The solution was stirred for 3 h to ensure that the mixture would evenly disperse in the solution. After this, an appropriate amount of transition metal chlorides MCl_2 (M= Ni, Co, Fe) was added to the solution. Then the solution was stirred again for half an hour. Finally, the whole solution was poured into a Teflon-lined stainless steel autoclave. The autoclave was maintained at 80-200 ^{0}C for 12-48 h. After it was cooled to room-temperature naturally, the solution was filtered. The obtained precipitate was washed with distilled H_2O, absolute alcohol several times, and then dried in a vacuum at 60 ^{0}C for 1 h.

1.2.4 Microemulsions:

The technique of chemical reactions in microemulsions to produce nanoparticles has been widely used now a days [31]. Microemulsions are thermodynamically stable systems composed of two immiscible liquids (usually, water and oil) and a surfactant. Droplets of water-in-oil (W/O) or oil-in-water (O/W) are stabilized by surfactants when

small amounts of water or oil are used, respectively. The size of the droplets can be controlled very precisely just by changing the ratio R = [water or oil] / [surfactant] in the nanometer range. These nanodroplets can be used as nanoreactors to carry out chemical reactions [32, 33].

The main idea of the microemulsion technique consists of mixing two reactants (A and B) in two identical microemulsions. After mixing both microemulsions, the droplets collide and interchange the reactants. Then the reaction can take place inside the nanoreactors. As a variation of this procedure [34], one of the reactants can be introduced in a solution into a microemulsion carrying the other reactant; or can be added directly to the microemulsions as a solid, liquid or gas. The most commonly used method of synthesis is to use two similar microemulsions containing the reactants [35].

Agostiano et al. [36] used this technique for the preparation CdS nano particles from water-in-oil microemulsion. The water-in-oil microemulsion system was composed of Cetyltrimethylammonium bromide (CTAB) as surfactant, pentanol as cosurfactant, n-hexane as oil phase, and reactant solution as aqueous phase. Microemulsions at [CTAB] = 0.1 M and molar ratio between water and surfactant (W_o) =5 were prepared by weighing in a volumetric flask the appropriate amount of surfactant, alcohol, n-hexane and water content. CdS nano particles were prepared by rapidly mixing equal volumes of two micellar solutions containing cadmium and sulphide salts, introduced in the microemulsions as aqueous solutions (Fig 1.1). Due to the dynamic properties of the reverse micelles the reactions occurs in few seconds and immediately after mixing the micellar solutions, CdS nano particles are formed.

All the methods providing the preparation of oxide nano powders involve the direct synthesis of small particles under conditions preventing them from growing. In the case of aluminum oxide, all the known physicochemical methods of its preparation including gas- and liquid- phase reactions, sol-gel processes, electrical explosion of wires lead to the formation of an amorphous or metastable gamma-modification [37]. An alternative way to prepare nanocrystalline α-Al_2O_3 is evidently the comminution of its coarse powder. However, the studies using high-energy mills [38] showed that for both wet and dry grinding there is some limit, evaluated on the basis of specific surface area and equal to approximately 40nm for $\alpha-Al_2O_3$. After this limit size is reached, further grinding again leads to the growth of particles.

For preparing nano alumina powders, heat treatment at 1100-1250^0 C is required. During thermal treatment it passes through the following series of phase transformation before conversion to α-Al_2O_3 [39]:

Hydrous alumina $\longrightarrow$ boehmite $\longrightarrow$ δ $\longrightarrow$ β $\longrightarrow$ γ $\longrightarrow$ α

Auto Ignition processing [53] is a simple method for the preparation of nano alumina powders. In this method by heat treatment at around 500-600^0 C only, nano crystalline α-Al_2O_3 powders were obtained.

1.3 Modification of nano particles using coupling agent:

Alumina particles contain –OH groups on its surface. In order to increase the reactivity of alumina or increase the adhesion between alumina particles and polymer matrix, the surface was modified using a coupling agent. Coupling agents are chemicals that are used to treat the surface of inorganic materials. These chemicals have two parts – one that combines with the surface chemically and another that is compatible with the

polymer [40]. One example, silane serve as common coupling agent and some of these are n-Amino propyltriethoxysilane [$(C_2H_5O)_3$-Si-$(CH_2)_3$-NH_2], n-Chloropropyltriethoxy silane [$(C_2H_5O)_3$-Si-$(CH_2)_3$-Cl], n-Cyanopropyltrimethoxy silane[$(CH_3O)_3$-Si-$(CH_2)_3$-CN] etc.,

The mechanism of reaction consists of two steps: in the first one the silane ester moiety is hydrolyzed to give:

$$(C_2H_5O)_3\text{-Si-}(CH_2)_3\text{-}NH_2 + 3H_2O \longrightarrow (OH)_3\text{-Si-}(CH_2)_3\text{-}NH_2 + C_2H_5OH$$

Which subsequently react with various OH groups of the surface,

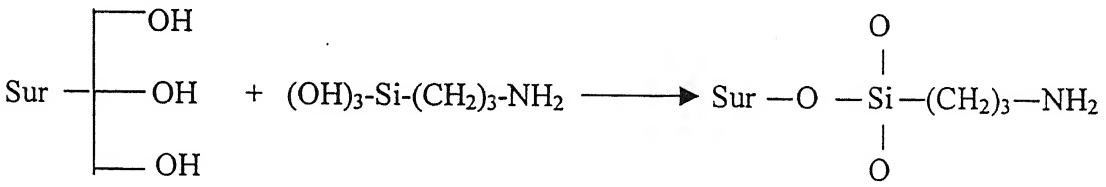

The net effect of this reaction is to give chemically bonded organic moiety to the inorganic surface. Another method is based on grafting polymeric molecules through covalent bonding to the hydroxyl groups existing on the particles. The advantage of the second procedure over the first one lies in the fact that the polymer grafted particles can be provided with desired properties through a proper selection of the species of the grafting monomers and the grafting conditions. In this way, the structure-property relationships of the nano composites can be tailored on purpose.

1.4 Different Ways of Preparing Polymer Nano Composites:

Making good samples of polymer matrix nano composites is a challenging area that draws considerable effort. There were a variety of processing techniques to make polymer matrix nano composites. These include melt mixing, insitu polymerization.

Vollenberg and Heikens [41] were able to produce good nano composite samples by thoroughly mixing filler particles with polymer matrix. The polymer matrices used in these experiments were polystyrene, styrene-acrylonitrile copolymer polycarbonate and polypropylene. The inclusions were alumina beads 35nm and 400nm in size and glass beads 4, 30, or 100μm in diameter. The volume fraction of particles ranged from 0 to 25%. Sample preparation consisted of dissolving polymers in polar solvent and mixing in the beads for several hours. The mixture was then poured over a large surface to allow the solvent to evaporate and it was subsequently dried under a vacuum at 100^0C. This mixture involved 30% volume fraction of particles and the pure polymer was then added to samples to achieve the desired particle volume fractions.

Chan et al. [42] made nano composites with polypropylene matrix and calcium carbonate ($CaCO_3$) through melt mixing of the components. First the components were dried in an oven at 120^0C and then cooled to the room temperature. The polypropylene was mixed first with an anti-oxidant. The $CaCO_3$ nano particles, which were 44nm in diameter, were then added slowly and mixing continued for a fixed time after all the particles were added. This technique produced good, reasonably well-dispersed samples at lower filler volume fractions, 4.8% and 9.2%, but aggregation was found at a higher volume fraction, 13.2%.

Poly urethane-silica nano composites have been made by Petrovic et al. [43] by mixing the silica with polyol. The mixture was then cured with diisocyanate at 100^0c for 16 h in presence of 0.1% catalyst Cocure 55 and subsequently poured into a mold. The particles were spherical with an average diameter of 12nm and had narrow

size distribution (10-20nm). Good samples were produced at 10%, 20%, 30% and 40% filler weight fraction, but the 50% filler weight fraction sample did not cure completely.

Rong et al. [44] grafted monomers made of styrene to surround the particles to produce better dispersion. They also used isotactic polypropylene as the matrix and SiO_2 as inclusions which were approximately 7nm in size. The particles were heated first to remove any water absorbed on the surface. Then, they were mixed with one of the monomers and solvent. This mixture was then irradiated and the solvent was removed. Samples were then made by adding polypropylene, tumble mixing, compounding and extruding. This technique produced samples with out aggregation and, in addition, greatly increased the particle-polymer matrix interfacial interaction.

Insitu polymerization is another technique that has been used to make polymer matrix nano composites [45, 46, 47]. It is a method in which particles are dispersed first in the monomer and then the mixture is polymerized. In Yang et al. [45], nano composites with polyamide-6 matrix and silica inclusions were produced by first drying the particles to remove any water absorbed on the surface. Then the particles were mixed with ε-caproamide and concurrently a suitable polymerization initiator was added. The mixture was then polymerized at a high temperature under nitrogen, this technique produced well-dispersed samples when the inclusions were around 50nm in size, but aggregation occurred for smaller particles around 12nm in size [47]. This was most likely due to the increased surface energy for the smaller particles, which, in the absence of a stabilizer, favored further particle segregation.

Li et al. [48] used a unique approach to prepare high density polyethylene (HDPE) – polypropylene nano composites. Seventy-five percent weight

HDPE and 25% polypropylene were melt-mixed and extruded into tapes. These tapes were then cut into shorter pieces and melt-processes by either extrusion or compression molding. This produced a nano composite with HDPE as the matrix and polypropylene fibrils ranging from 30 to 150nm in diameter.

For clay nano composites, the specific choice of processing steps depends on the final morphology required in the composite, i.e, exfoliated or intercalated form [49, 50]. In the intercalated form, matrix polymer molecules are introduced between the ordered layers of clay resulting in an increase in the interlayer spacing, but still maintaining the order. On the other hand, in an exfoliated form, clay layers are separated and are distributed with in matrix. Intercalated nano composites are generally formed by melt blending or by insitu polymerization. Exfoliation ability depends on the nature of clay, blending process, and the agents used for curing. The final structure of clay composite has a wide range of variations, depending on the degree of intercalation and exfoliation.

Thus in general, there is no single procedure that is followed for making polymer matrix nano composites. As seen from the above mentioned summary the most important factor to consider in the preparation of polymer nano composites is the requirement of good particle dispersion in the polymer matrix.

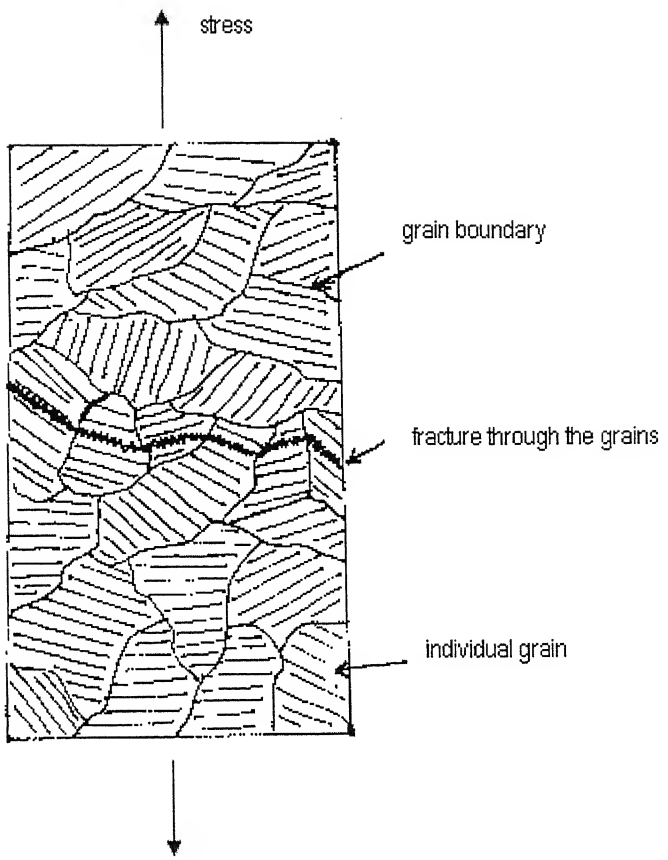

Fig 1.1 schematic diagram showing transgranular fracture

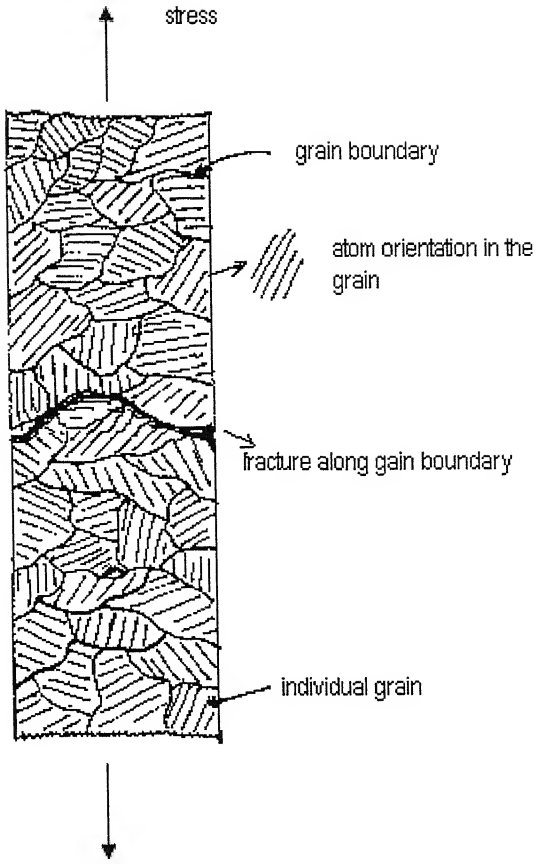

Fig 1.2 schematic diagram showing Intergranular fracture

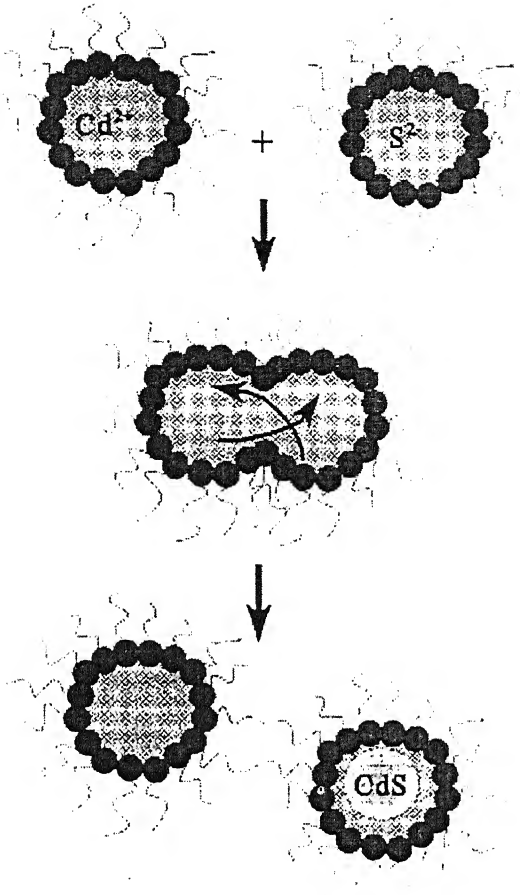

Fig 1.3 Pictorial representation of the synthesis of nano CdS in reverse micelles

Chapter 2
EXPERIMENTAL DETAILS

2.1 Preparation of plate like nano alpha alumina particles

The hydrous alumina was prepared by adding $NH_3 .H_2O$ solution (0.2mol l^{-1}) slowly to a rapidly stirred $Al(NO_3)_3.9H_2O$ solution (4.5 mol l^{-1}). PEG (molecular weight 1000) solution was used as disperant to prevent the powder from agglomerating [51]. When the slurry pH was adjusted to 9.0, the precipitate was aged in the container with constant stirring intensively for 1 h without removing the solution, then the slurry was filtered and kept without washing and dried at 70^0C for 24 h. After that, the dried gel was milled with alcohol by adding ZnF_2 (2 wt. %) in high purity alumina mediums for 24 h and then dried at 50^0C for 12 h. The gel was calcined at different temperature for 1 h with fast or slow heating rate. A flow chart of the process was given in Fig 2.1

2.2 Preparation of Nano Alumina Particles

Alumina nano particles were prepared by auto ignition reaction of aluminum nitrate and urea [52]. In order to take the advantage of the exothermic reaction, it is important to arrive at the proper composition of the oxidizer/fuel mixture. In the present case, aluminum nitrate was used as the oxidizer and urea was chosen as the fuel. The total oxidizing and reducing valencies of the reactants were adjusted according to the procedure developed by Jain et al. [53]. In order to ensure that the energy released by the reaction is the maximum, they used a quantity termed as the equivalent ratio and defined it as the ratio of the total oxidizing valency to the total reducing valency. A stoichiometric composition is defined as the composition where this ratio is equal to 1. For the present

compositions, the equivalent ratio of aluminum nitrate to urea was determined to be 3.0. It can be determined as follows:

The valencies of the oxidizing elements Cl and O have been taken as positive and those of fuel elements C and H as negative, with N taken as neutral [54]. The valency of element O is +2, H is -1, N is 0 and C is -4.

The total reducing valency of fuel (urea) = -4 + 2 + [0+2 (-1)] 2 = -6.

The total oxidizing valency of oxidizer (aluminum nitrate) = 0 + [0 +3(+2)] 3+9[2(-1) +2]

= 18.

Therefore, the Equivalent ratio = 18/6 = 3.0

In the typical experiment, the constituents were mixed with water in a paste-like consistency in a beaker and placed in a furnace maintained at 500^0C. The paste melts and eventually undergoes decomposition with evolution of gases resulting in a foamed structure, which then ignites. The entire combustion is over within a few minutes. The as processed foams were crushed into powders and was ready for use in experiments.

2.3 Synthesis of Methacrylol Chloride

Methacrylol chloride was prepared by the reaction of methacrylic acid (48.5ml, 0.5gmole) with equal number of moles of thionyl chloride (98ml, 0.5gmole)[55].Initially methacrylic acid (48.5ml) was taken in a conical flask and to this, thionyl chloride (98ml) taken in a dropping funnel, was added dropwise. The reaction was carried out at 0^0C for 2 hours and the product was methacrylol chloride formed according to the reaction.

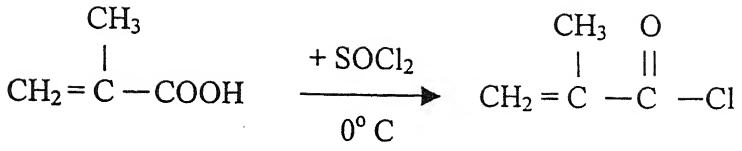

2.4 Synthesis of Methacrylol Isocyanate

Methacrylol Isocyanate was prepared by the reaction of sodium azide (35g, 0.538gmole) with equal number of moles of methacrylic chloride in presence of dry benzene (20ml) [56]. Initially sodium azide (35g) and dry benzene (20ml), were taken in a conical flask and to this methacrylol chloride (92ml), taken in a dropping funnel was added dropwise. The reaction was carried out at 0^0C for 8 hours, after which it is filtered. The permeate was methacrylol isocyanate formed according to the reaction.

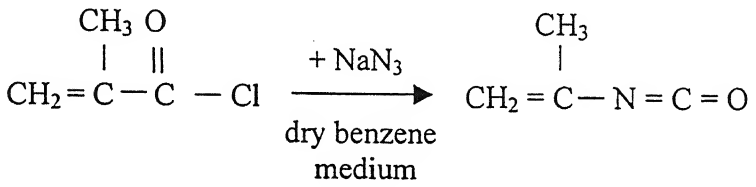

2.5 Chemical modification of nano alumina particles

Nano alumina particles obtained from step 2 were taken in a conical flask to which methacrylol isocyanate was added. The mixture was stirred at 0^0C for 6-8 hours. The final product was dried in an oven at 60^0C. The dry material was then crushed into powders. The powder thus obtained was modified nano alumina. The photograph of alumina particles and modified alumina particles was given in fig. 2.2

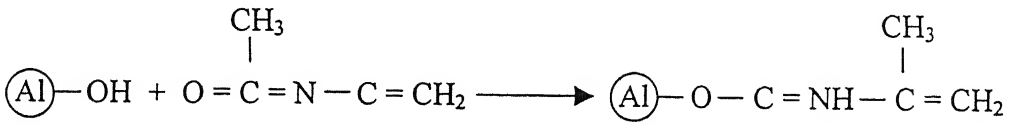

2.6 Preparation of PMMA Nano Composite:

2.6.1 Materials

The methylmethacrylate (MMA) and ethyleneglycoldimethacrylate (EGDM) were washed to remove the inhibitor. Benzoylperoxide (BPO) and azobisisobutyronitrile (AIBN) were recrystallized from methanol. Dimethylaniline (DMA) was used as received. Modified nano alumina particles as received from step 2.5.

The monomer as obtained consists of inhibitors (Monomethyl Ether Hydroquinone, pyrocatechol) to prevent it from polymerizing. In order to remove the inhibitor, the monomer was washed initially 3 times with 5% NaOH and then finally 3 more times with distilled water.

150 ml of methanol and known amount of BPO (20g) were taken in a beaker. The contents in the beaker were heated upto 40^0C for 30 minutes. The top methanol layer is taken into a conical flask and cooled at around 0^0C for 3-4 hrs, during which the BPO gets recrystallized. The BPO crystals were then filtered from methanol.

Similarly 150 ml of methanol and known amount of AIBN (20g) were taken in a beaker. The contents in the beaker were heated upto 40^0C for 30 minutes. The top methanol layer is taken into a conical flask and cooled at around 0^0C for 3-4 hrs, during which the AIBN gets recrystallized. The AIBN crystals were then filtered from methanol.

2.6.2 Preparation of Polymer Nano Composite

Here the monomer (MMA) was polymerized using the following dual initiating system [57]. A mixture of MMA (20g, 0.2gmoles), BPO (0.26g, 0.1074gmoles), AIBN (0.14g, 0.085gmoles) and an accelerator DMA (0.082g, $6.789X10^{-4}$ gmoles) were mixed in a conical flask and then heated gently in a water bath up to around 60^0C. Once the viscosity

of the polymer has changed, non settling modified nano alumina particles (2%by wt., 0.4g) were added to the polymer. Then the polymerization mixture was well stirred for 1-2 hrs, so that the nano particles were completely mixed. To the final mixture a cross linking agent, EGDM (2g, 0.0101gmoles) was added and the mixture was then stirred for 5 more minutes.

Two thin (2mm thick) PMMA sheets were taken and the final well mixed polymer syrup was applied between the PMMA sheets in the form of thin uniform layer. Then the sheets were baked, by keeping them in an oven at around 60^0C. The photograph of PMMA sheets with polymer and with syrup containing non settling nano alumina particles was given in fig 2.3.The impact strength of the attached polymer sheets were tested using drop weight impact testing machine and bullet firing machine.

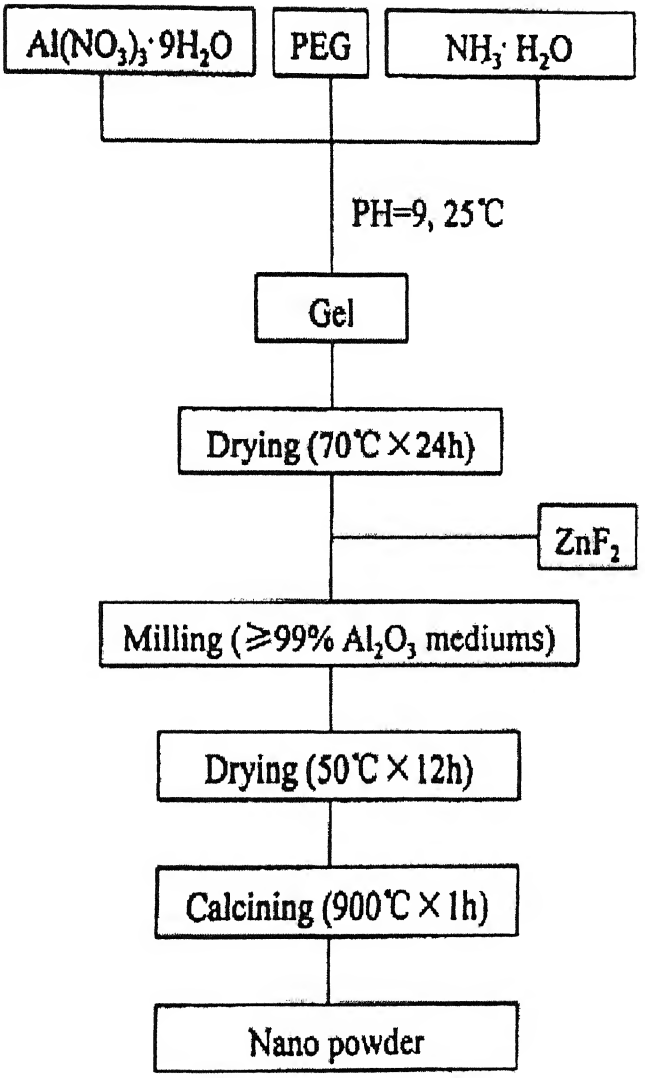

Fig 2.1 Flow sheet representing the process for the preparation of plate like nano alumina particles.

(a)

(b)

Fig 2.2 Photograph showing (a)nano alumina particles, (b) modified nano alumina particles

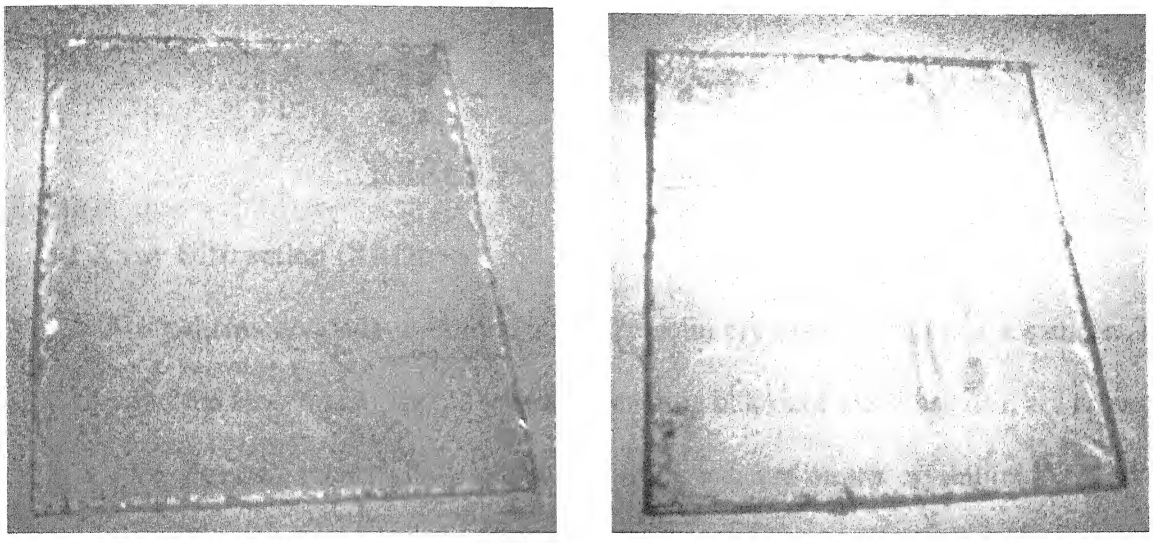

(a) (b)

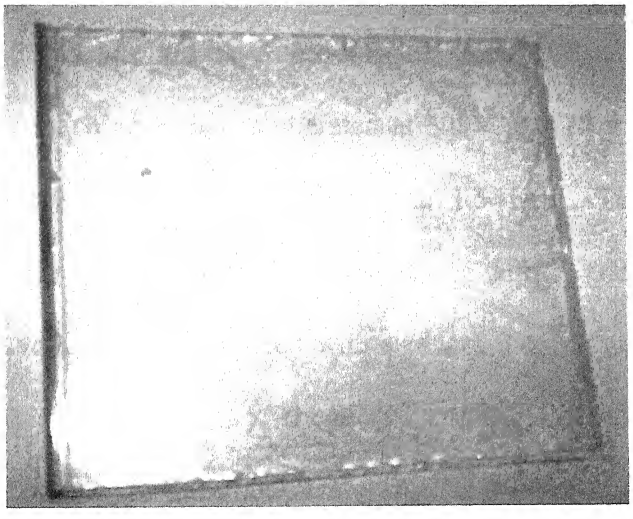

(c)

Fig 2.3 Photograph showing (a) empty PMMA sheets, (b) PMMA sheets with polymer,(c)PMMA sheets with polymer syrup containing non settling nano particles.

Chapter 3

RESULTS AND DISCUSSION

3.1 X ray Diffraction (XRD):

An X-ray diffraction was used to identify the solid crystalline phases in a sample. The atoms and the ions, which are the chemical building blocks of the substance, are arranged in a three dimensional structure. When X-rays are incident on the crystalline solid, these are diffracted due to elastic scattering of the ray quanta on the electrons of those chemical building blocks of the material. The lattice structure, therefore, can be related to the resulting diffraction pattern. We have used a Reich Seifert (Germany) Iso Debye Flex X-ray diffractometer machine which is operated at 30kV and 20 mA by using Ni-filtered monochromatic CuK< radiation of wave length 1.5418^0A. The resulting diffraction patterns were recorded on a PC using a software along with'd' and intensity values.

The 'd' values were compared with standard data, to analyze the nature of the compound, i.e., its crystal geometry, chemical formula, lattice parameters. Fig 3.1, 3.2 shows the XRD pattern for nano alumina and modified nano alumina particles. From these, the "d" values have been recorded in table 3.1 and 3.3. We have also obtained the "d" values and the plane indices of standard <-alumina from powder diffraction file [58]. The match between these two has been within 1% and one is justified to call the product as <-alumina. The comparison of tables 3.1 and 3.3 show that the "d" values do not change very much and it is possible to conclude that the surface modification has not changed the crystal structure.

3.1.1 Finding crystal size of nano alumina and modified nano alumina:

Scherrer [56] has derived an expression for broadening of X-ray diffraction peaks for small crystalline sizes as follows [59]:

$$B_{crystalline} = \frac{k\lambda}{L\cos\theta} \quad \text{----------} \quad (3.1)$$

The lattice strain in the material also causes broadening of the diffraction peaks, which can be represented by the relationship:

$$B_{strain} = \eta \tan\theta \quad \text{----------} \quad (3.2)$$

B_r represents the full width at half maxima (FWHM) and is due to the combined effects of crystalline size and lattice strain. The expression for B_r is given to be:

$$B_r = B_{crystalline} + B_{strain} = \frac{k\lambda}{L\cos\theta} + \lambda\tan\theta \quad \text{----------} \quad (3.3)$$

By plotting a graph between $B_r\cos\theta$ and $\sin\theta$, from the intercept, we can get the value of $\frac{k\lambda}{L}$.

Where,

λ is the wavelength of X-rays used, $\lambda_{Cu\,K\alpha} = 1.54\ A^0$, θ is Bragg angle, L the average crystal size, k is a constant, whose value varies from 0.89 and 1.39. For small cubic crystals of uniform size, its value is 0.94.

Fig 3.3 shows the graph of $B_r\cos\theta$ and $\sin\theta$ for nano alumina and modified nano alumina particles. From the graph of $B_r\cos\theta$ and $\sin\theta$ and using equation (3.3), one determines the average crystal size of nano alumina as 28.5 nm and the average crystal size of modified nano alumina as 36.4 nm.

3.2 Surface area measurement:

The surface area was measured by single point BET method, utilizing the physisorption of nitrogen gas at 77K. The measurement was carried out on a Micrometerics Pulse Chemisorb 2705, USA which works on a dynamic adsorption technique. The alumina samples were first prepared by heating up to 423K for 20 min in an inert atmosphere to remove any adsorbed species from the alumina surface. Helium gas at a flow rate of 15ml/min was then used as the inert gas and then the test gas consisting of 30 mol% nitrogen in N_2-He mixture was passed through the sample. After stabilization of the flow, the sample was immersed in a bath of liquid nitrogen to condense the nitrogen in the nano particles. Then the condensed nitrogen gas was desorbed by bringing the sample to the room temperature by immersing it in a fresh water bath. The BET surface area for the nano alumina particle was this way determined to be 117.23 m^2/g

3.3 Transmission Electron Microscopy (TEM):

The samples for TEM were prepared by adding a small amount of the product to 50ml of methanol, and the carbon dispersed in methanol by ultrasonication. A copper grid was taken and a film deposited on one side of the grid by 2% polyvinyl formal (formvar) dissolved in 1,2-dichloroethane. After this, the grid was dried under either 100W bulb light or room temperature for 2-3 hours. After settling of all large particles in the suspension of carbon in methanol previously prepared, a small amount of solution was introduced by a dropper nearly at the interface of the light and dark regions of methanol on the film coated side of the grid. Commercial grids on which the formvar film was already formed were also used with the identical procedure except that the film formation step was not required. Grids were dried for 2-3 hours under ambient conditions and were

studied with JEOL Transmission (JEM2000FX) operating at 100kV voltage. Fig 3.4 shows the TEM image of the nano alumina particles from which the particle size of nano alumina from TEM analysis was determined to be 40nm which is found close to the particle size estimated from XRD analysis.

3.4 Fourier Transform Infrared (FT-IR) Analysis:

The FT-IR spectra of alumina (formed by procedure of section 2.2), modified alumina (formed by procedure of section 2, methacrylol chloride and methacrylol isocyanate have been analyzed. Fig 3.5 shows the FT-IR of alumina. It shows the presence of –OH at 3433.15 cm^{-1} (lit. [60] 3100-3700cm^{-1}). Fig 3.6 shows the FT-IR of alumina modified with methacrylol isocyanate. It shows the presence of –NH at 3412.47 cm^{-1} (lit. 3300-3500 cm^{-1}) and $-CH_2$ at 2358.17 cm^{-1} (lit. 2300-3000 cm^{-1}) and C=C at 1630 cm^{-1} (lit. 1450-1650 cm^{-1}). Fig 3.7 shows the FT-IR of methacrylol chloride formed by the reaction of methacrylol acid and thionyl chloride. It shows the presence of C=O at 1790.82 cm^{-1} (lit. 1650-1870 cm^{-1}) and C=C at 1455.88 cm^{-1} (lit. 1450-1650 cm^{-1}) and $-CH_3$ at 2989.45 cm^{-1} (lit. 2800-3000 cm^{-1}) and C-Cl at 744.39 cm^{-1} (lit. 400-800 cm^{-1}). Fig 3.8 shows the FT-IR of methacrylol isocyanate synthesized by the reaction of methacrylol chloride and sodium azide in dry benzene medium. It shows the presence of C=N at 1558.98 cm^{-1} (lit. 1550-1650 cm^{-1}) and C=C at 1455.67 cm^{-1} (lit. 1450-1650 cm^{-1}) and N=C=O at 2927.43 cm^{-1}.

3.5 Thermo Gravimetric Analysis (TGA):

The TGA analysis of unmodified and modified nano alumina particles were carried out in a temperature range of 40-900^{0}C under nitrogen atmosphere. Fig 3.9, 3.10 shows the TGA of nano alumina and the modified nano alumina particles. It can be seen from these

figures that there is 10% weight loss for nano alumina particles at 900^0C and 23% weight loss for modified nano alumina particles at 900^0C. It can be seen that for modified nano alumina particles, the TGA shows a slight break at around 331^0C, which indicates the loss of methacrylol isocyanate layer. Fig 3.11, 3.12 shows the DTA of nano alumina and the modified nano alumina.

3.6 Application Procedure:

The polymer syrup formed by mixing 2% non settling nano alumina particles with PMMA, was applied in between two PMMA sheets of 2mm thickness each by two methods. The first one, by hand method, in which the polymer syrup was applied at one end of the PMMA sheet, then using a thin paint brush, it was spread over the entire sheet, doing the same procedure to second sheet, then the sheets were attached and hold tightly using bench wise. In the second method an air sprayer was used in which the polymer syrup was taken into the cup arrangement in the sprayer, then by applying pressure from back side, the syrup was sprayed onto the two PMMA sheets, then the sheets were attached and hold tightly using bench wise. The advantage of using second method over the first one was that with the sprayer, the polymer syrup can be applied uniformly over the PMMA sheets. Fig 3.13 shows the picture of PMMA sheets made via hand made technique and spray technique.

3.7 Bubble Formation between PMMA Sheets:

After applying the polymer syrup containing non settling nano particles in between the PMMA sheets, if the composite sheets were kept for 4-5 hrs and then heated at around 60^0C, there was formation of bubbles in between the sheets, which can be clearly seen from fig 3.14a. One remedy to this problem was to cook the PMMA sheets immediately

after holding tightly using bench wise for 15 minutes. Fig 3.14b shows the picture of PMMA sheets in which there was no formation of bubbles, when heated immediately.

3.8 Testing of specimen in the Bullet Firing Machine:

It consists of a gun assembly, in which the bullets are propelled to desired velocities by using compressed N_2 gas. The speed of the bullet can be fixed within a reasonable range and can be monitored by photoelectric bulbs. The schematic diagram is given in fig 3.15. The photograph of the bullet firing machine is given in fig 3.16.

The target is fixed to the frame of the bullet firing machine. Then the sequence of operation is thus followed by closing valves SC, SP, LV, LD and FL and opening valves FD. To fire the bullet, valves CV, SV were opened and valve FD was closed as referred in fig 3.15.

Here the bullet was fired with 9 J energy for PMMA sheets and 20 J for Polycarbonate sheets. From the kinetic energy equation,

$$E = \tfrac{1}{2} mv^2 \qquad \text{----------} \qquad (3.4)$$

Where, m is mass of bullet whose value is 4.73 g, v is velocity of bullet. From above equation, the value of v is found to be 91m/s for polycarbonate sheets and 62 m/s for PMMA sheets. After firing with this much velocity, the non joined sheets were completely shattered (see fig. 3.17a), as opposed to this, the sheets with polymer have 59% damaged area (see fig. 3.17b), and whereas the sheets with polymer syrup containing non settling nano particles has only 9.6% damaged area (see fig. 3.17c)

In case of Polycarbonate sheets, the non joined sheets were completely shattered (see fig. 3.18a), where as the sheets with polymer has 34% damaged area (see fig.3.18b),

where as the sheets with polymer syrup containing non settling nano particles showed no damaged area (see fig.3.18c).

3.9 Testing of specimen in the Vertical Drop Weight Impact Testing Machine:

It consists of a tup of weight 14.5 kg, which drops on to the specimen from a reasonable height. The maximum energy is 140 J and maximum height of the tup from the specimen is 1 m. the height from which the specimen has to drop can be calculated from potential energy equation given by:

$$E = mgh \qquad \text{----------} \qquad (3.5)$$

Where,

E is the potential energy with which the tup must drop, g is acceleration due to gravity, h is the height from which tup must drop. The machine is fully computerized and from PC we get the data of Force and Time. The photograph of Drop Weight Testing Machine is given in fig 3.19.

Here the PMMA sheets were tested with 3 J energy (h=211 cm) and Polycarbonate sheets with 6 J energy (h=422 cm) and recorded the variation of load with time.

Graphs 3.20, 3.21, 3.22 shows the variation of force with time for empty PMMA sheets, PMMA sheets with polymer and PMMA sheets with polymer syrup containing 2% non settling nano particles. From these graphs, the maximum load for empty PMMA sheets was found to be 55.66 Kg, the maximum load for PMMA sheets with polymer was found to be 90.82 Kg and the maximum load for PMMA sheets with polymer syrup containing non settling nano particles was found to be 166.99 Kg.

Graphs 3.23, 3.24, 3.25 shows the variation of force with time for empty poly carbonate sheets, poly carbonate sheets with polymer and poly carbonate sheets with polymer syrup containing 2% non settling nano particles. From these graphs, the maximum load for empty poly carbonate sheets was found to be 102.54 Kg, the maximum load for poly carbonate sheets with polymer was found to be 144.53 Kg and the maximum load for poly carbonate sheets with polymer syrup containing non settling nano particles was found to be 193.36 Kg.

Table 3.1: Analysis of the XRD pattern of the nano alumina particles recorded with Cu Kα radiation

Peak position (2θ)	'd' Value (theoretical)	'd' Value (experimental)	hkl plane indices
25.58	3.4793	3.482707	012
35.14	2.5523	2.553750	104
37.75	2.3791	2.382814	110
43.32	2.0850	2.088480	113
52.49	1.7400	1.743243	024
57.42	1.6011	1.604760	116
61.27	1.5100	1.513245	018
66.47	1.4039	1.407321	124

Table 3.2: Crystal structure data of Alumina

Property	Value
Crystal geometry	Trigonal
Chemical formula	α-Al_2O_3
Lattice parameter	a = b = 4.758 A^0 c = 12.991 A^0

Table 3.3: Analysis of the XRD pattern of the modified nano alumina particles recorded with Cu Kα radiation

Peak position (2θ)	'd' Value (theoretical)	'd' Value (experimental)	hkl plane indices
25.59	3.4793	3.480553	012
35.10	2.5523	2.556586	104
37.72	2.3791	2.385080	110
43.25	2.0850	2.091902	113
52.40	1.7400	1.745979	024
57.38	1.6011	1.605739	116
61.22	1.5100	1.514523	018
66.41	1.4039	1.408134	124

Table 3.4: Crystal structure data of Modified Alumina

Property	Value
Crystal geometry	Trigonal
Chemical formula	α-Al_2O_3
Lattice parameter	a = b = 4.758 A^0 c = 12.991 A^0

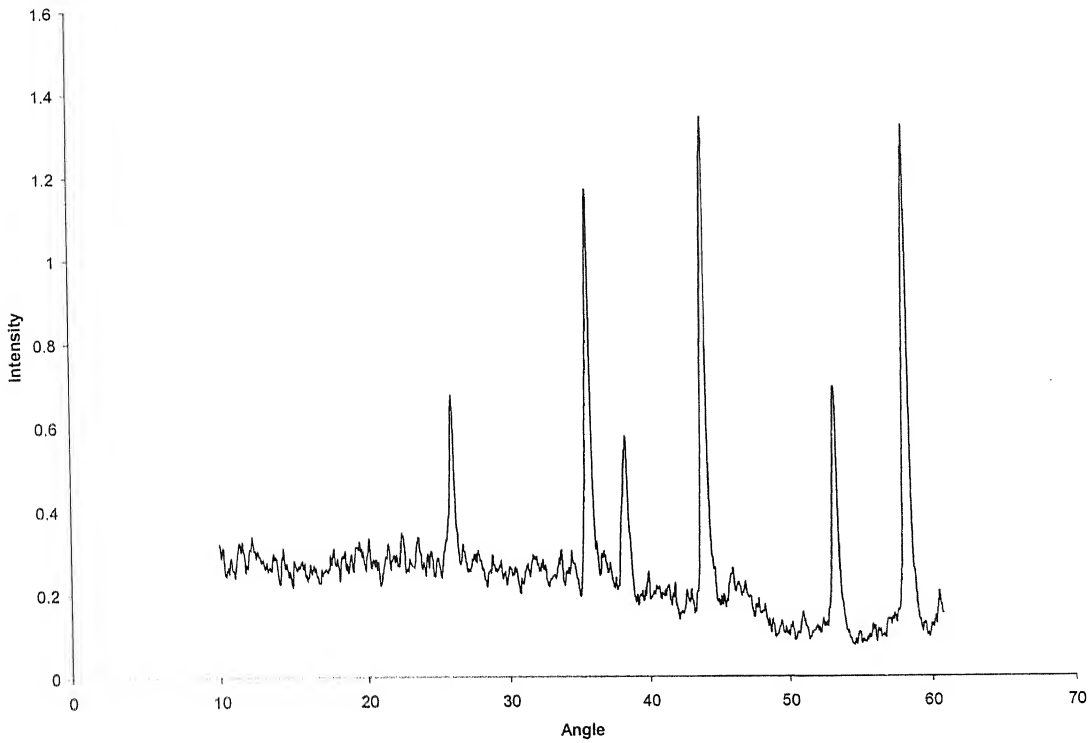

Fig 3.1: XRD pattern of nano alumina particles

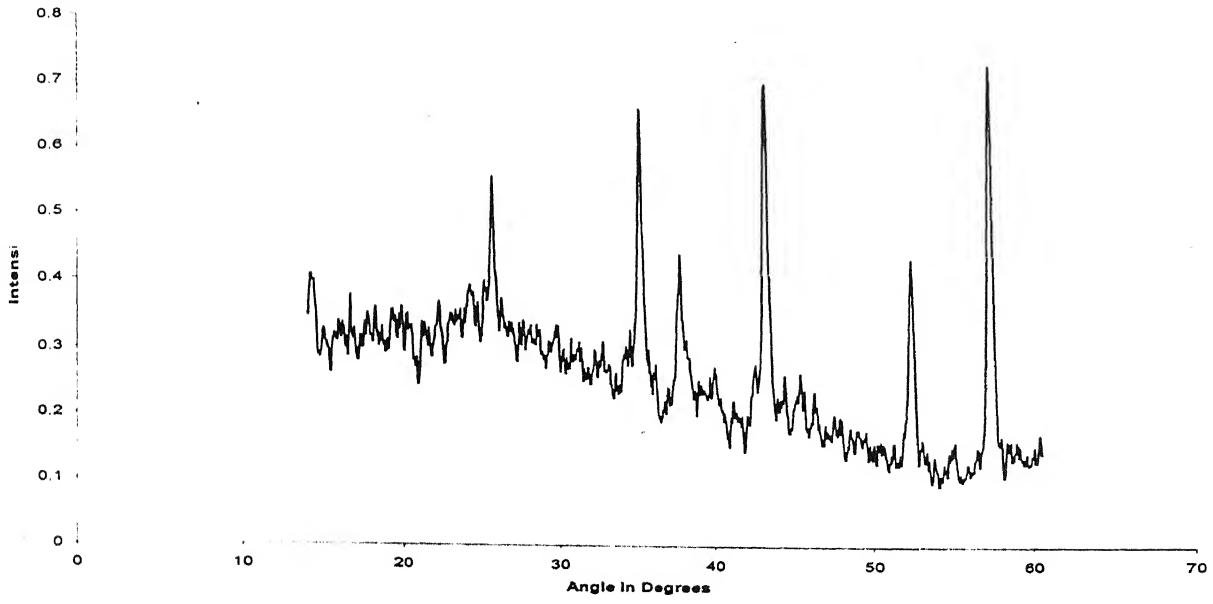

Fig 3.2: XRD pattern of modified nano alumina particles

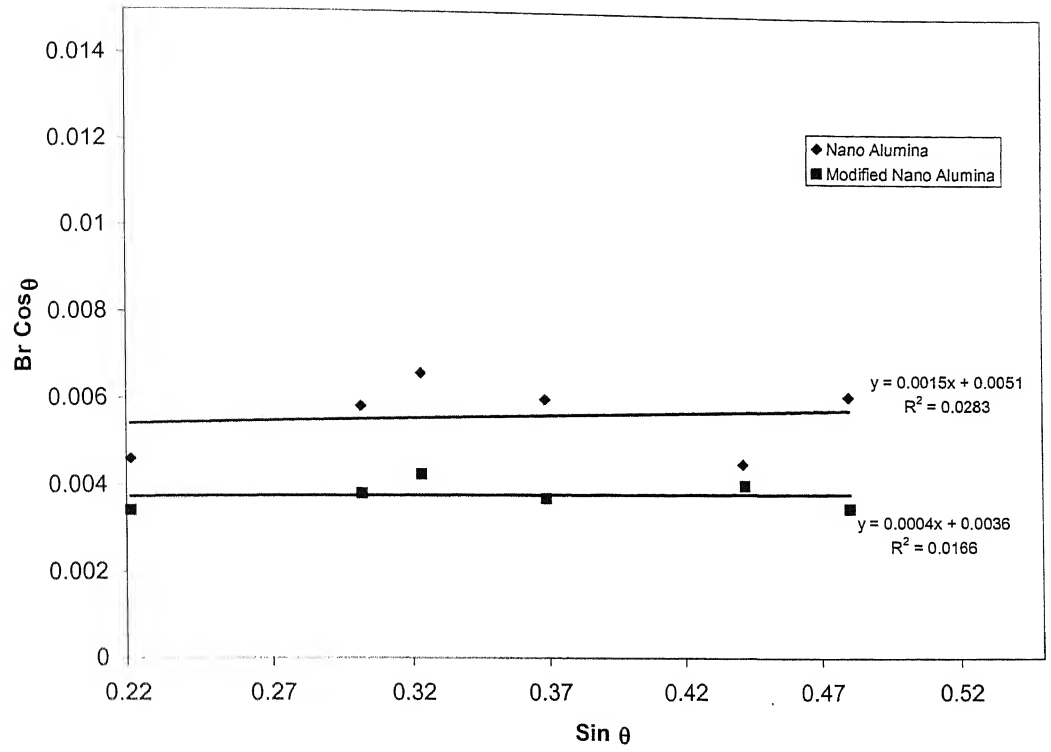

Fig 3.3 Graph between B_r Cos θ and Sin θ for nano alumina particles and modified nano alumina particles

Table 3.5 B_r Cos θ and Sinθ values for nano alumina and modified nano alumina

B_r Cosθ (nano alumina)	B_r Cosθ (modified nano alumina)	Sinθ (nano alumina)	Sinθ (modified nano alumina)
0.004593	0.003413	0.221463	0.22138
0.005826	0.003813	0.301538	0.3018
0.006596	0.004258	0.323257	0.3235
0.005996	0.003718	0.36853	0.3689
0.004531	0.004036	0.441508	0.44226
0.006114	0.003508	0.48007	0.480377

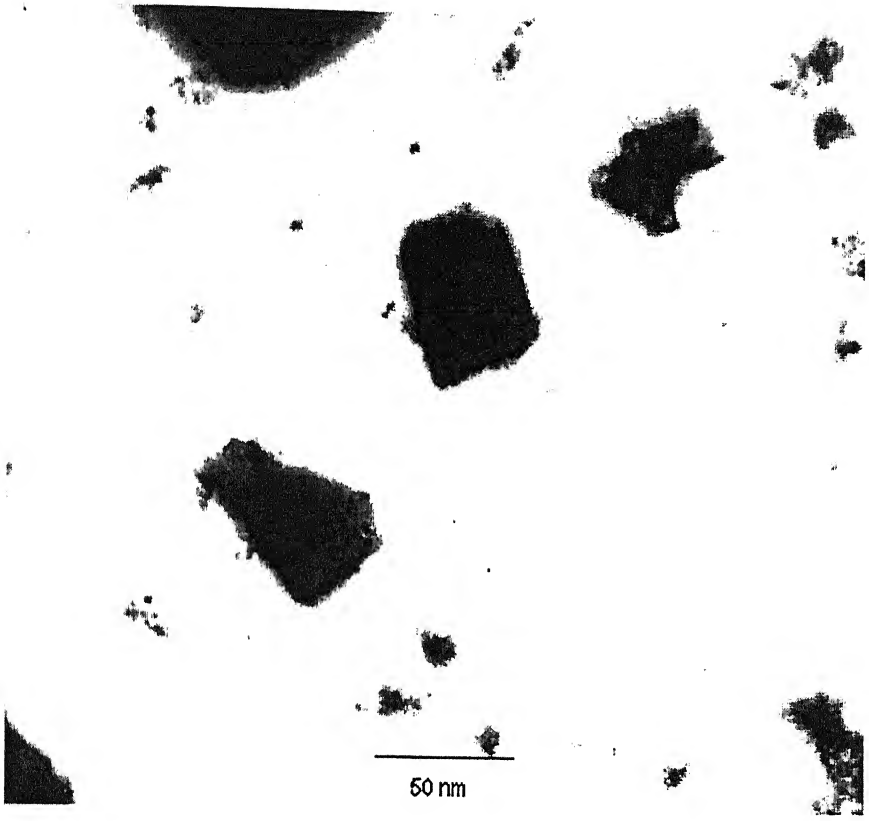

Fig 3.4 TEM image of nano alumina particles.

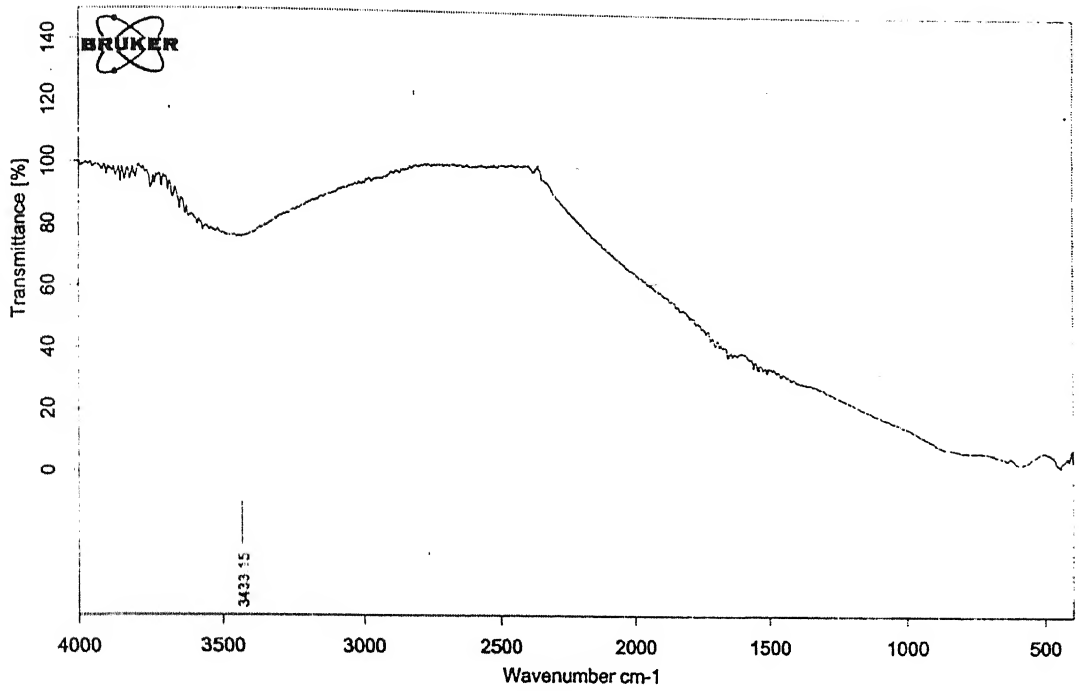

Fig 3.5 FT-IR analysis of nano alumina particles

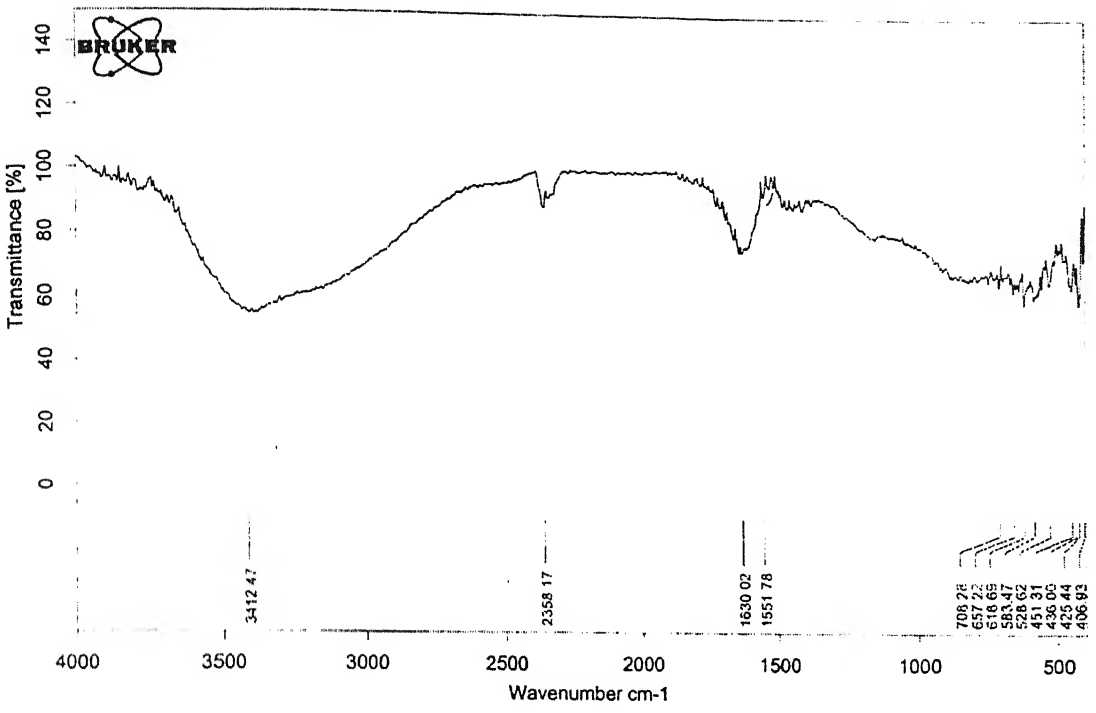

Fig 3.6 FT-IR analysis of modified nano alumina particles

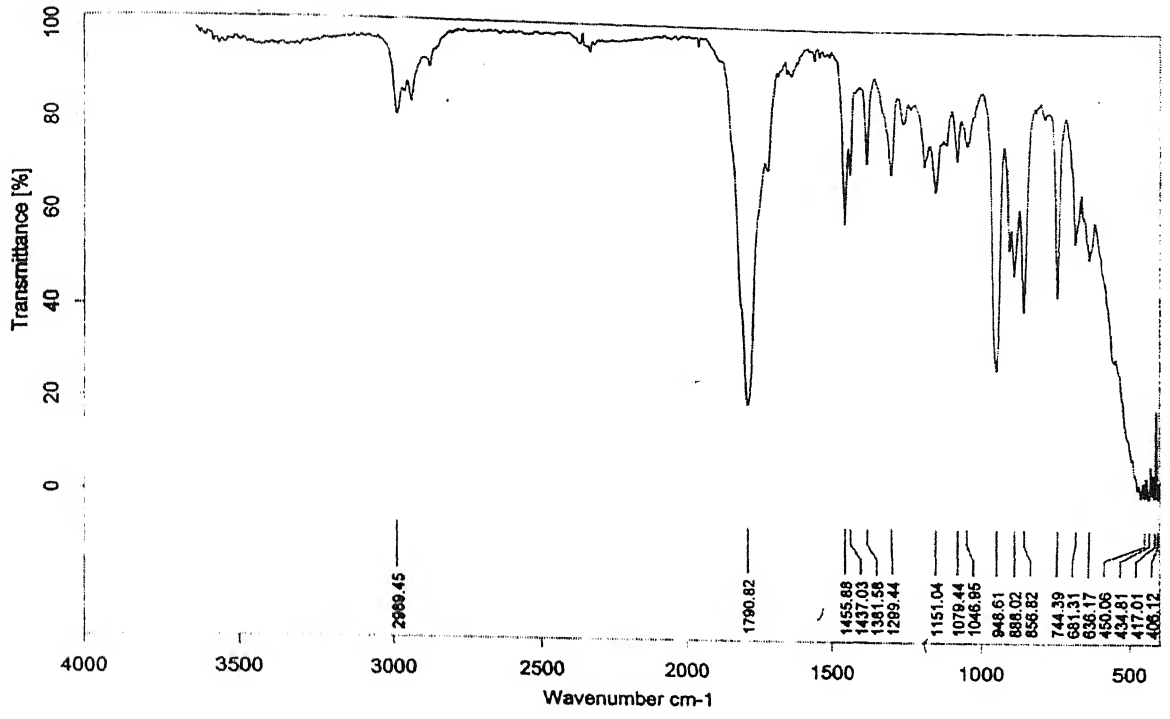

Fig 3.7 FT-IR analysis of Methacrylol chloride

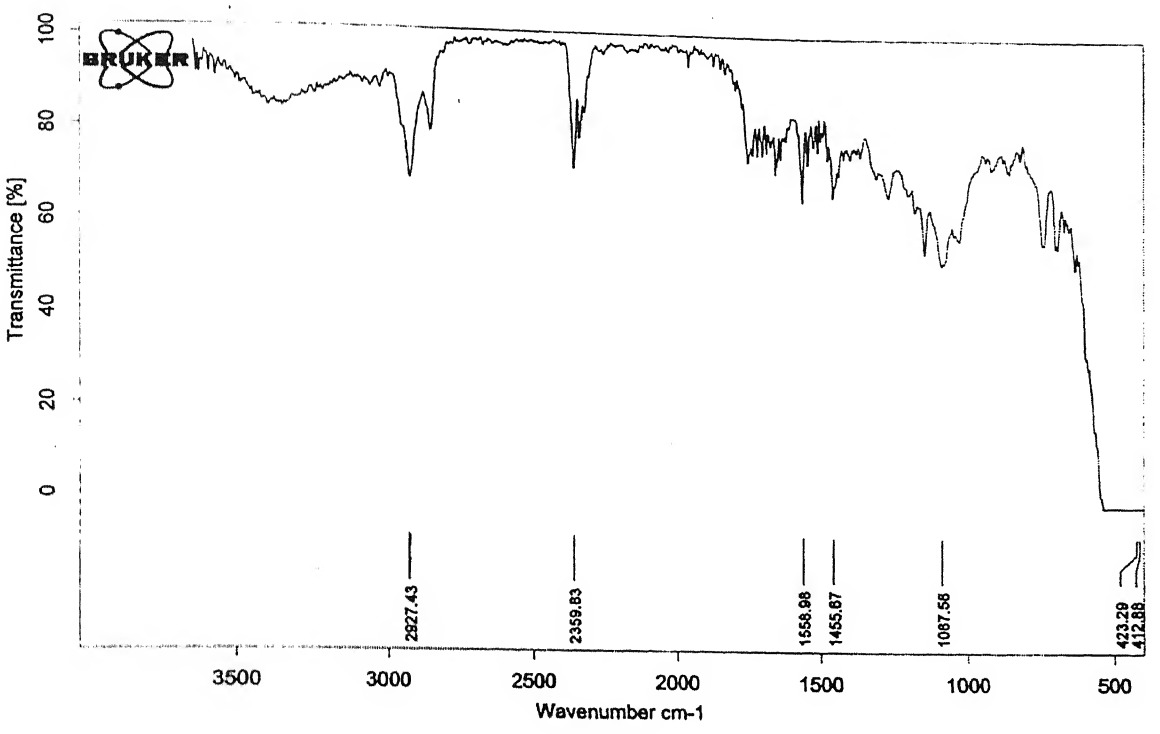

Fig 3.8 FT-IR analysis of Methacrylol isocyanate

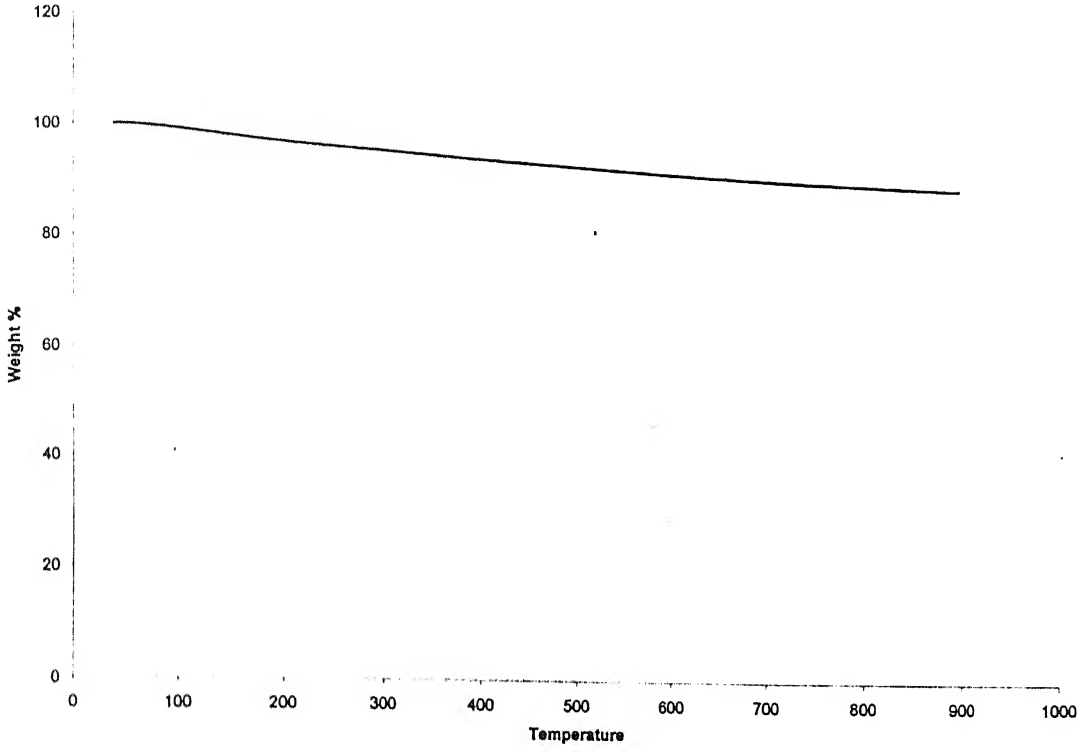

Fig 3.9 TGA graph of nano alumina particles

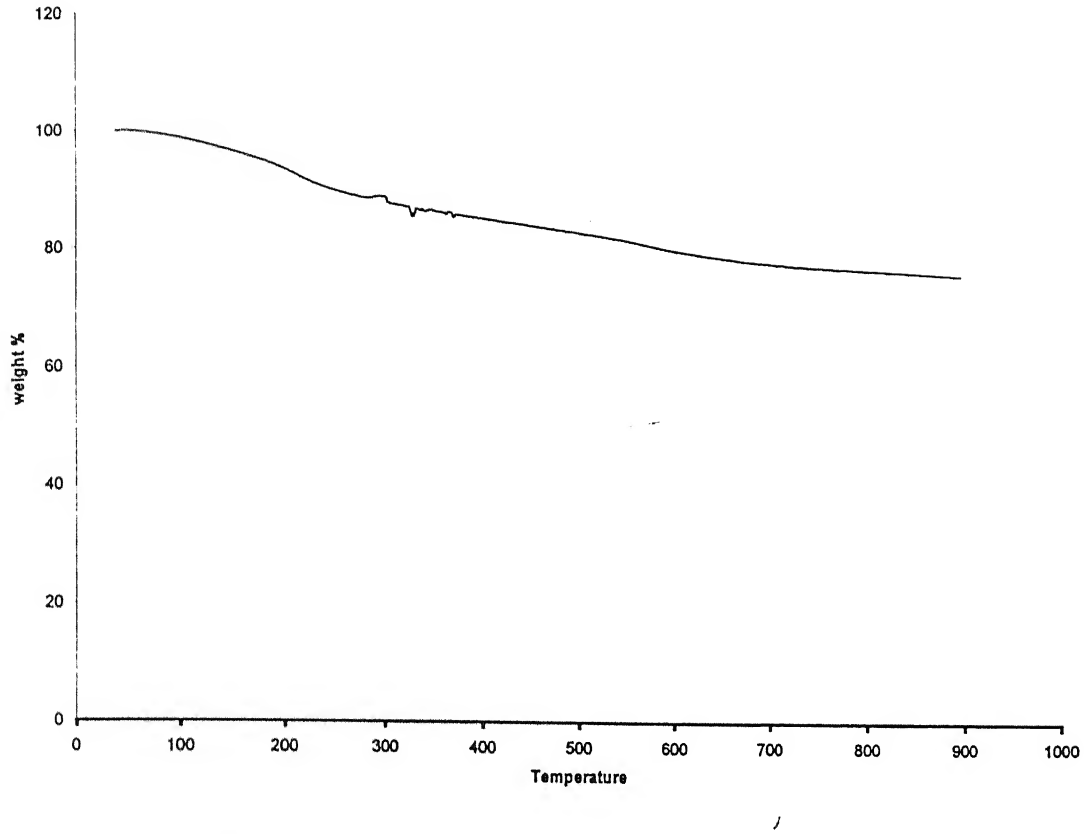

Fig 3.10 TGA graph of modified nano alumina particles

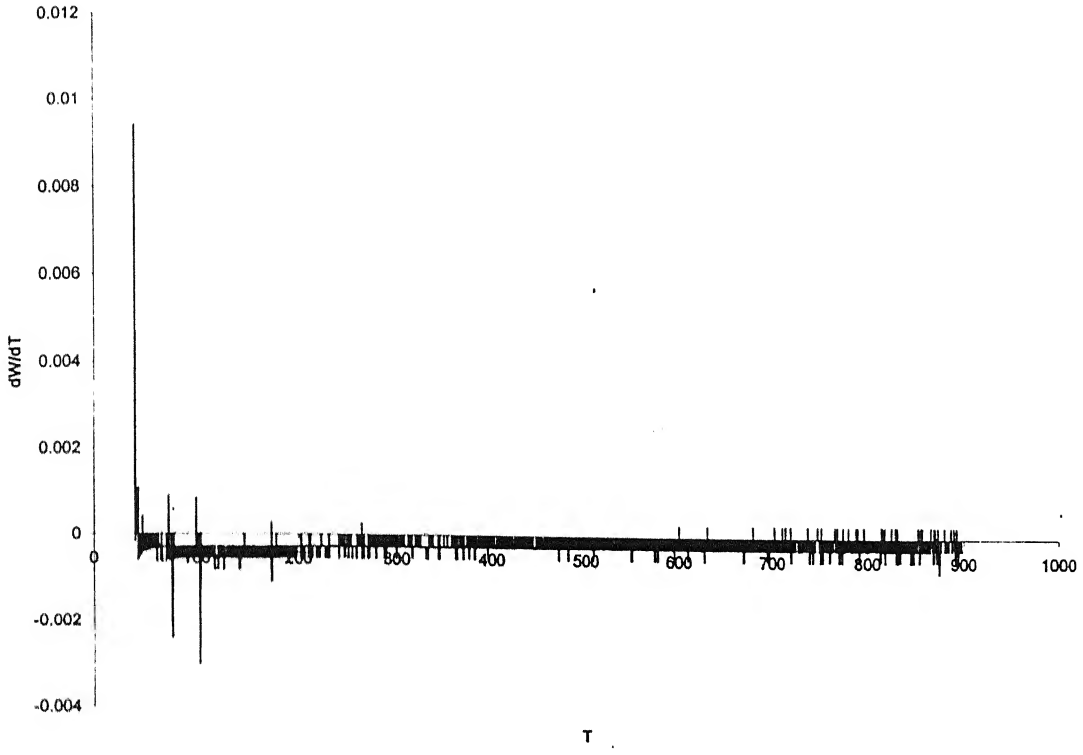

Fig 3.11 DTA graph of nano alumina particles

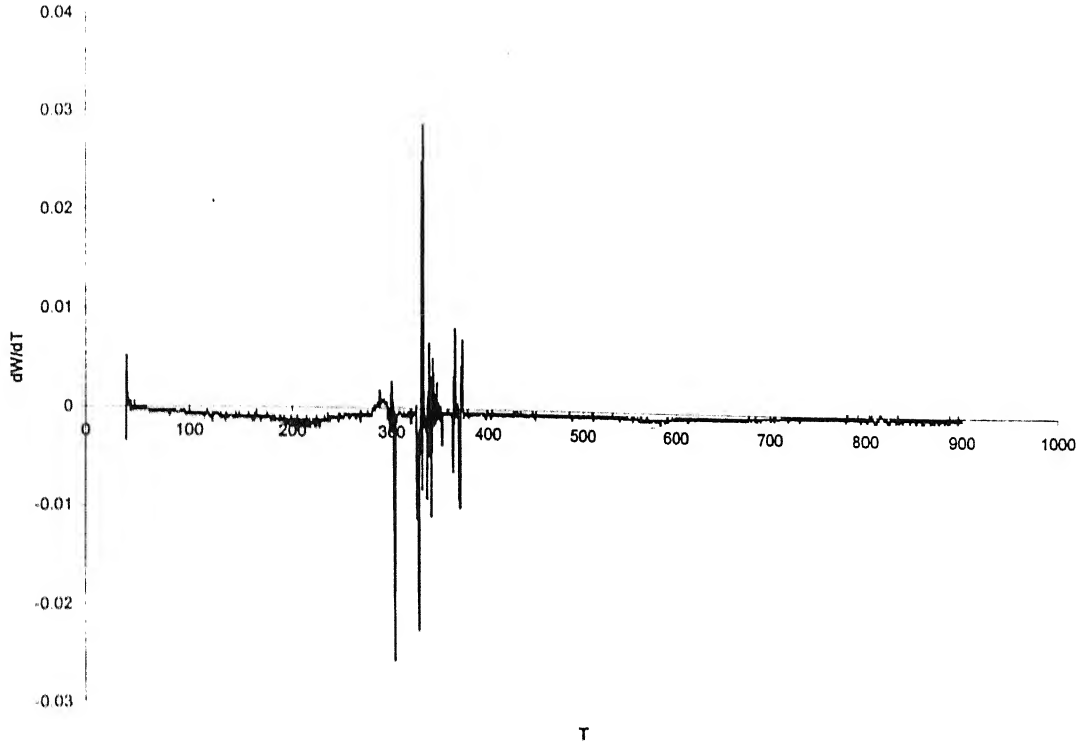

Fig 3.12 DTA graph of modified nano alumina particles

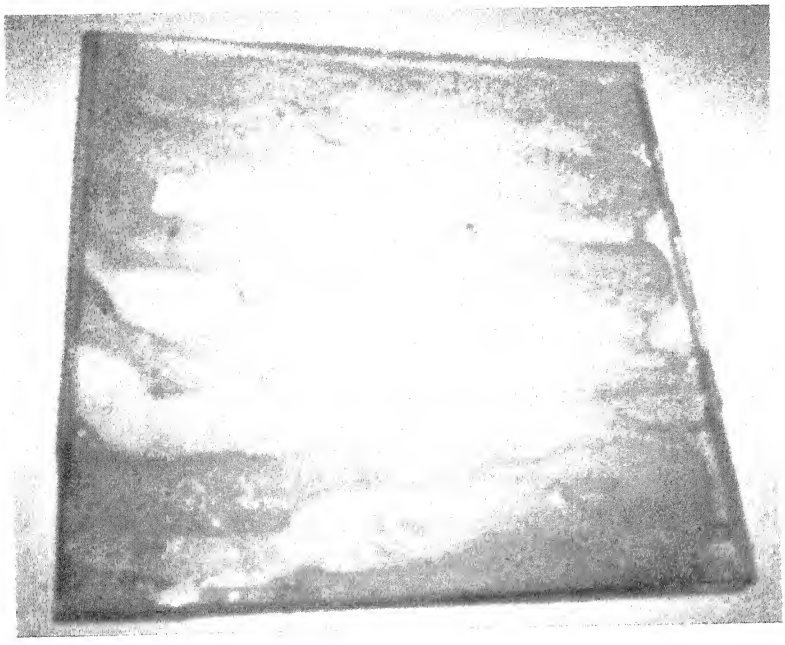

(a)

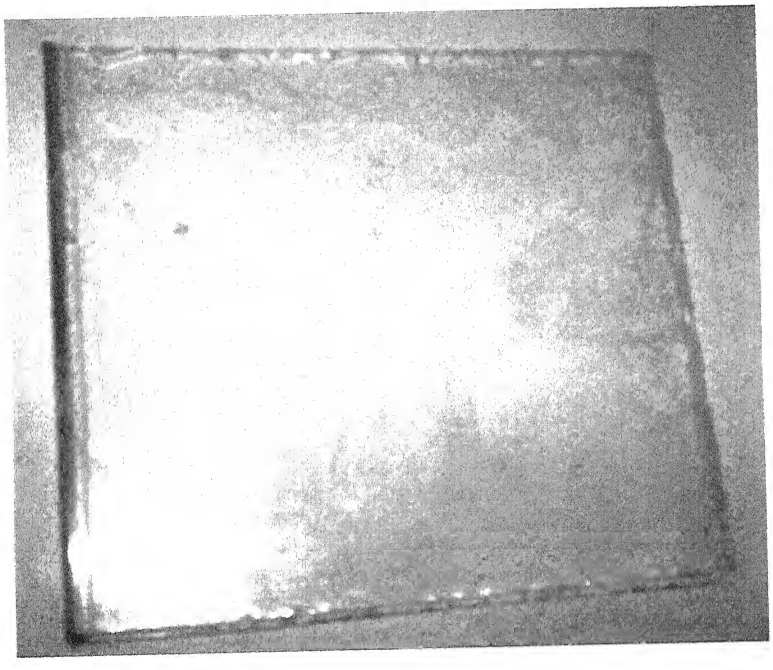

(b)

Fig 3.13 Photograph showing PMMA sheets each 2 mm thick and 12 cms x 12 cms dimension (a) with polymer syrup containing 2% non settling nano particles applied via hand made technique and (b) spray technique.

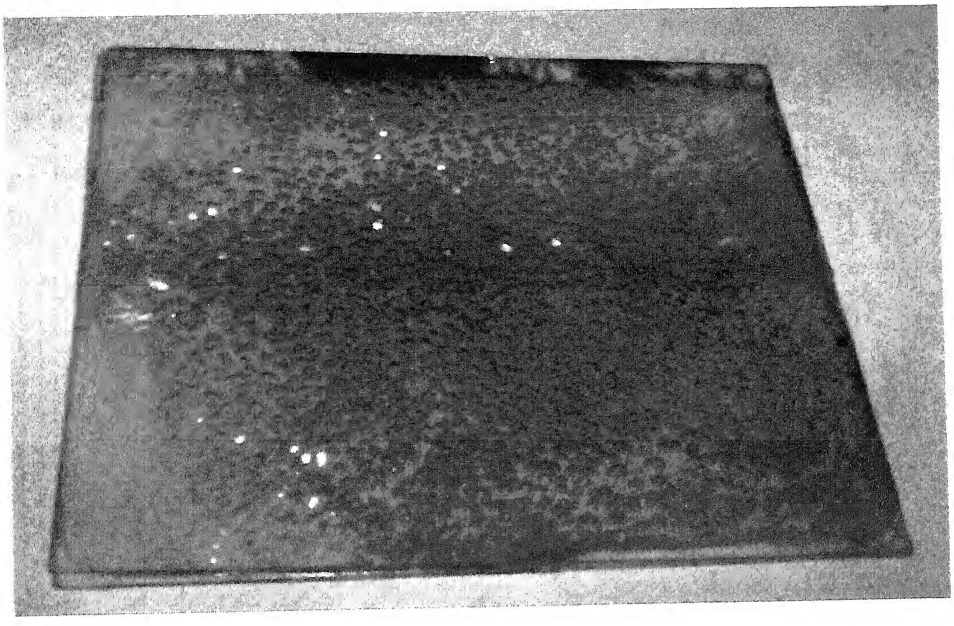

(a)

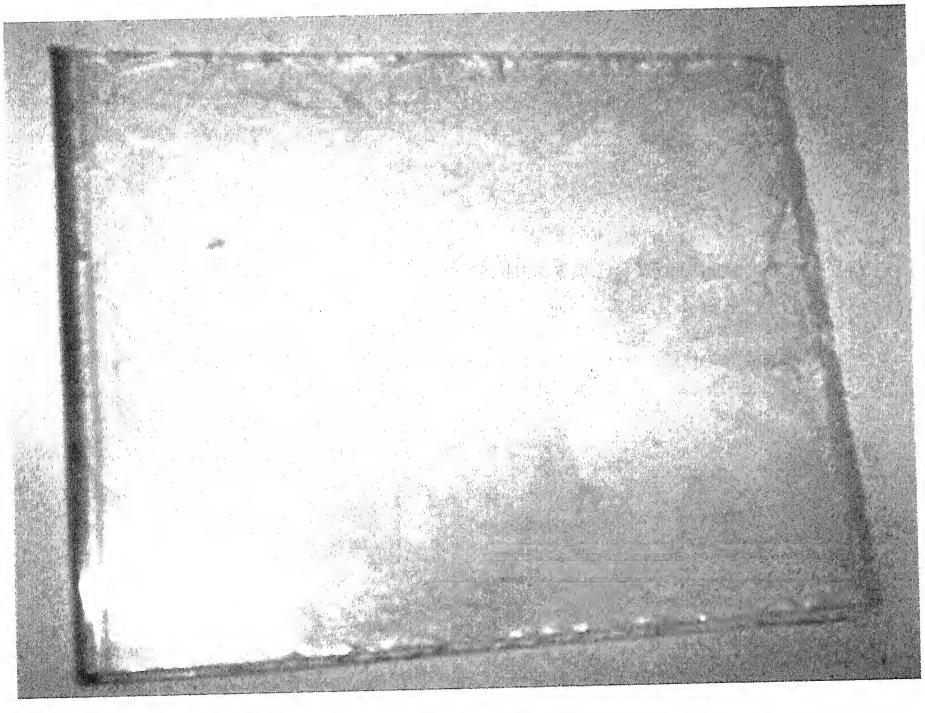

(b)

Fig 3.14 Photograph showing PMMA composite sheets of 2 mm thickness each and 12 cms x 12 cms dimension (a) with bubbles and (b) with out bubbles

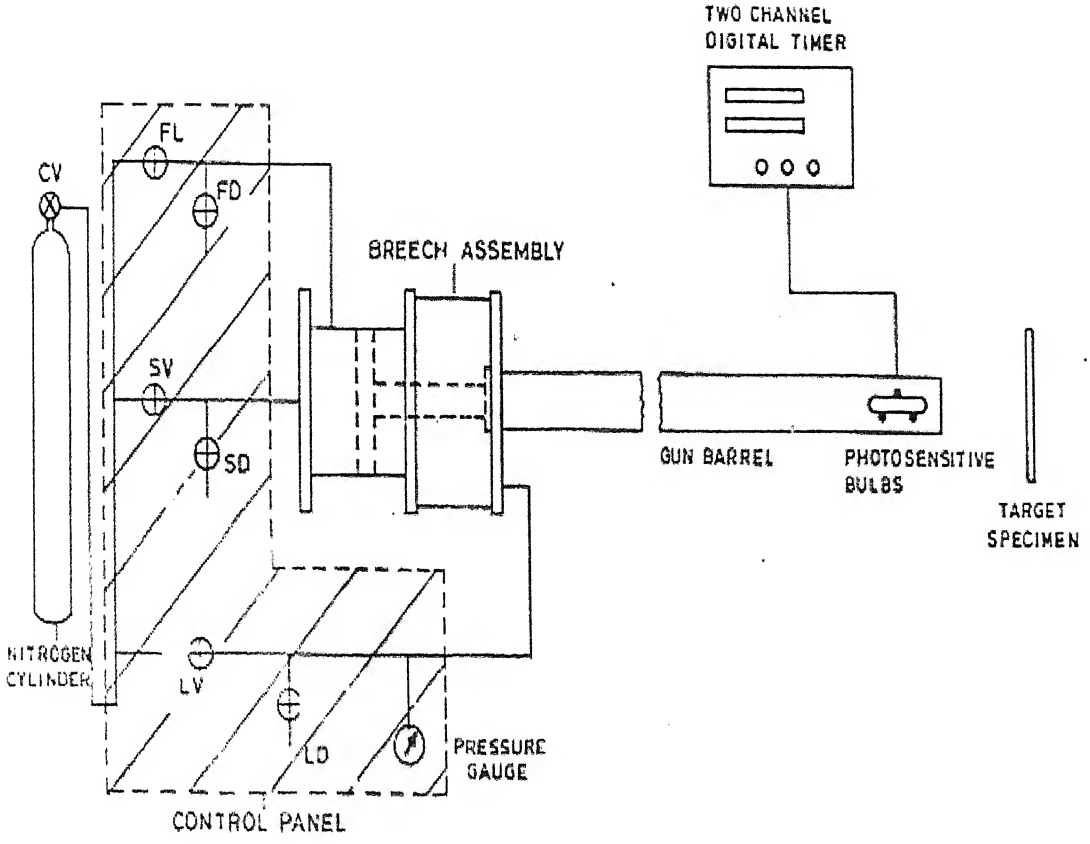

Fig 3.15 Schematic diagram of Bullet Firing Machine

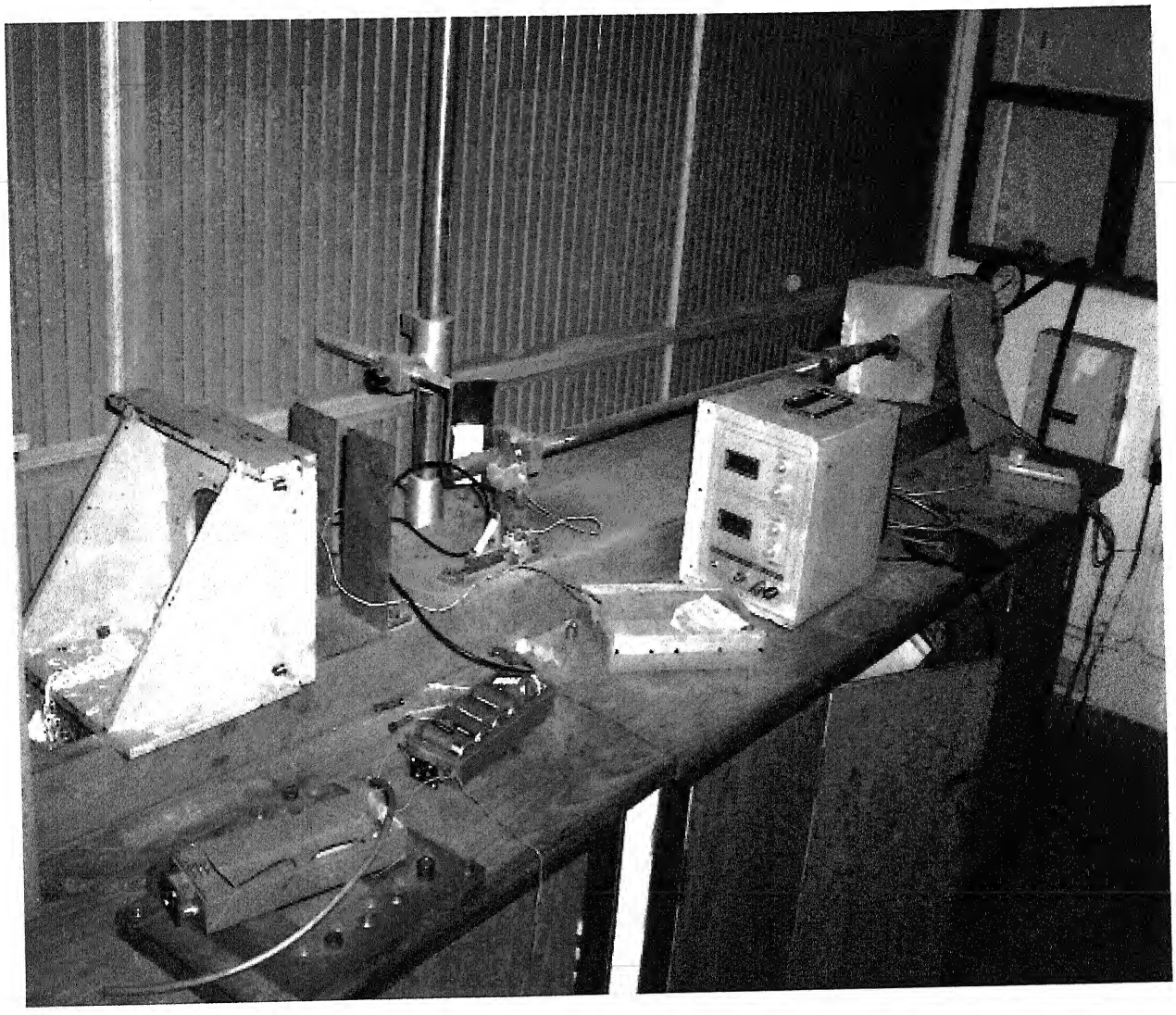

Fig 3.16 Photograph of Bullet Firing Machine

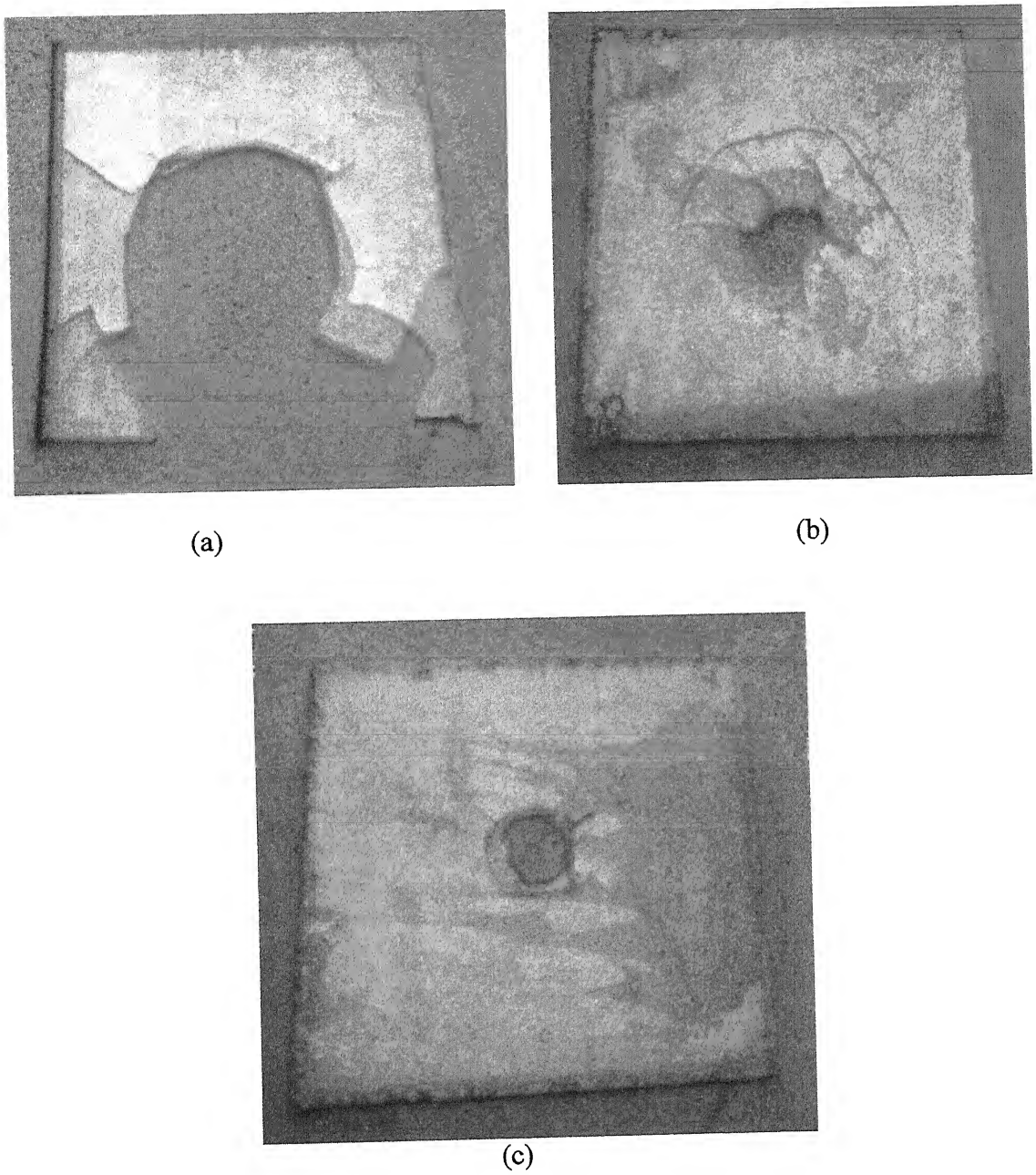

Fig 3.17 Photograph of PMMA sheets with 2 mm thickness each and 12 cms x 12 cms dimension after bullet firing (a) non joined, (b) with polymer, (c) with polymer syrup containing 2%non settling nano particles.

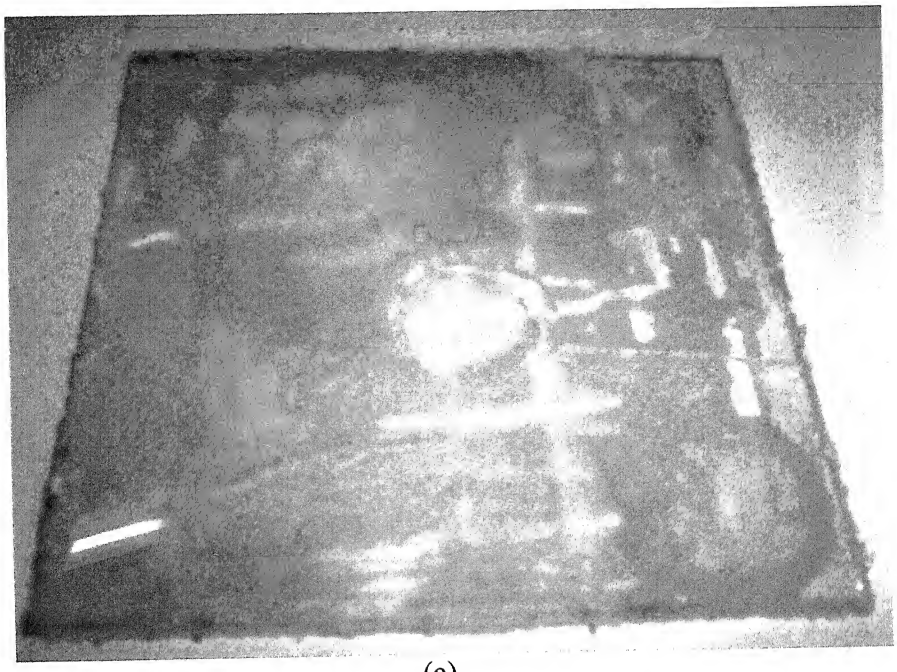

(a)

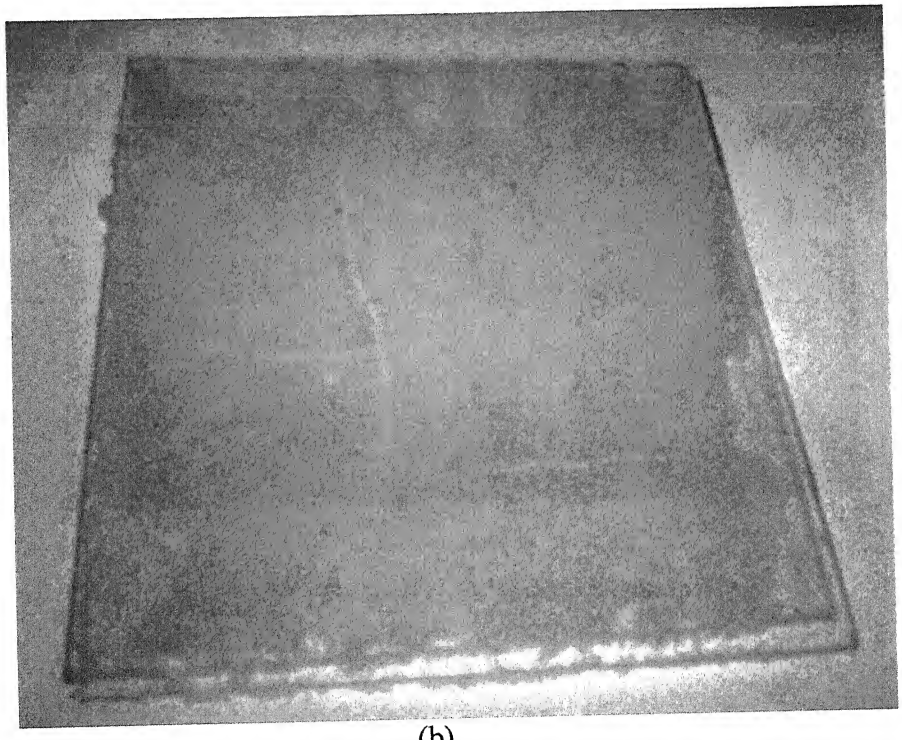

(b)

Fig 3.18 Photograph of PolyCarbonate sheets with 2 mm thickness and 12 cms x 12 cms dimension (a) with polymer (b) with polymer syrup containing 2% non settling nano particles.

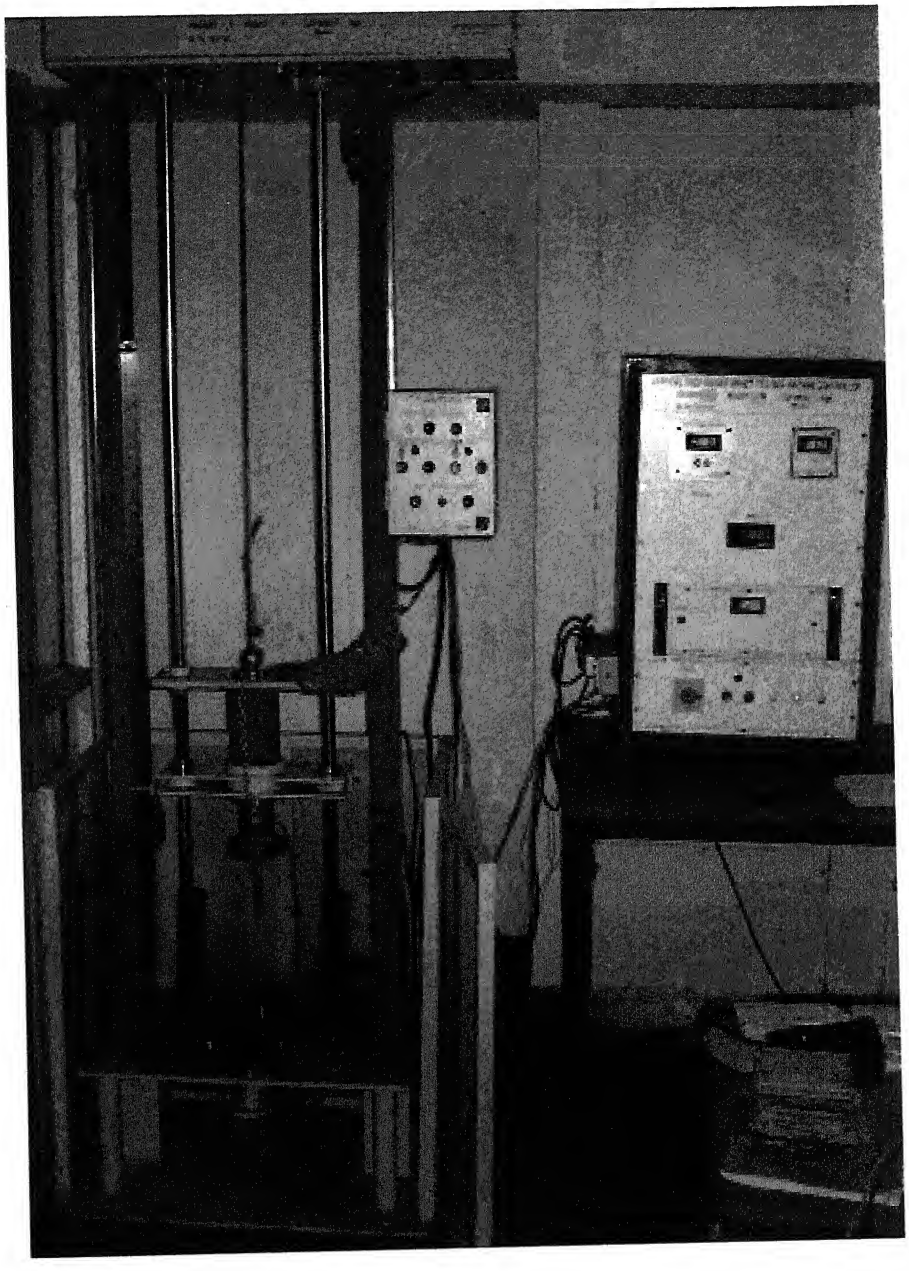

Fig 3.19 Photograph of Drop Weight Impact Testing Machine

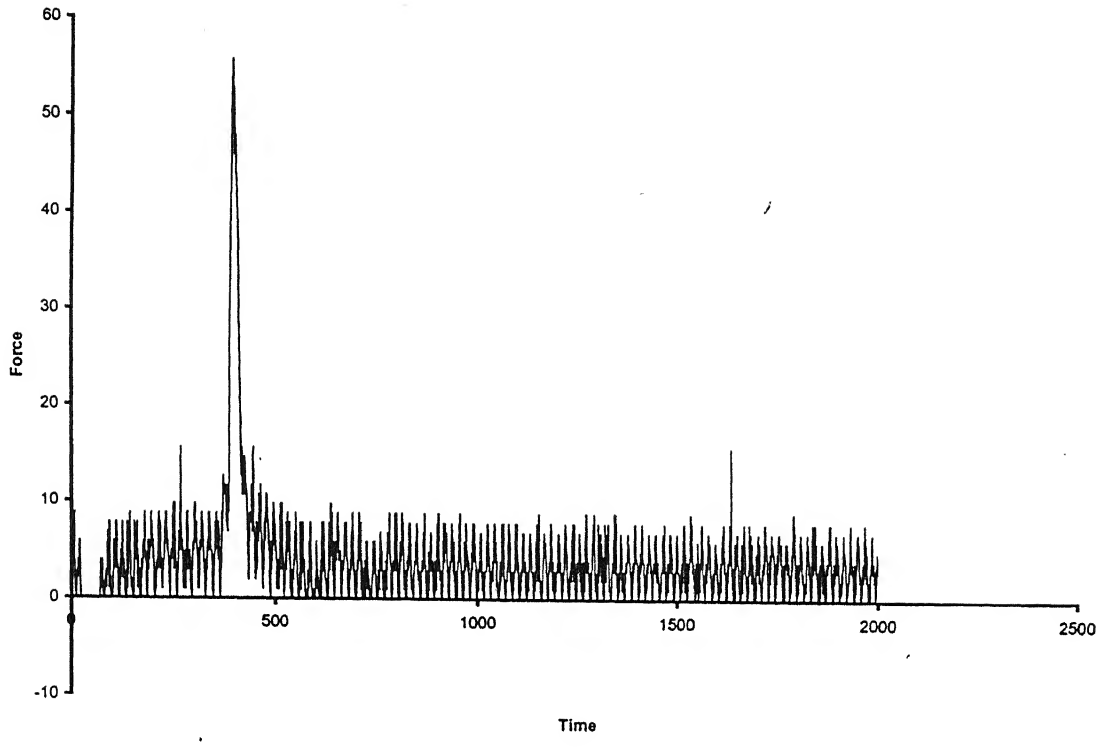

Fig 3.20 Graph of Force and Time during drop weight impact testing for empty PMMA sheets.

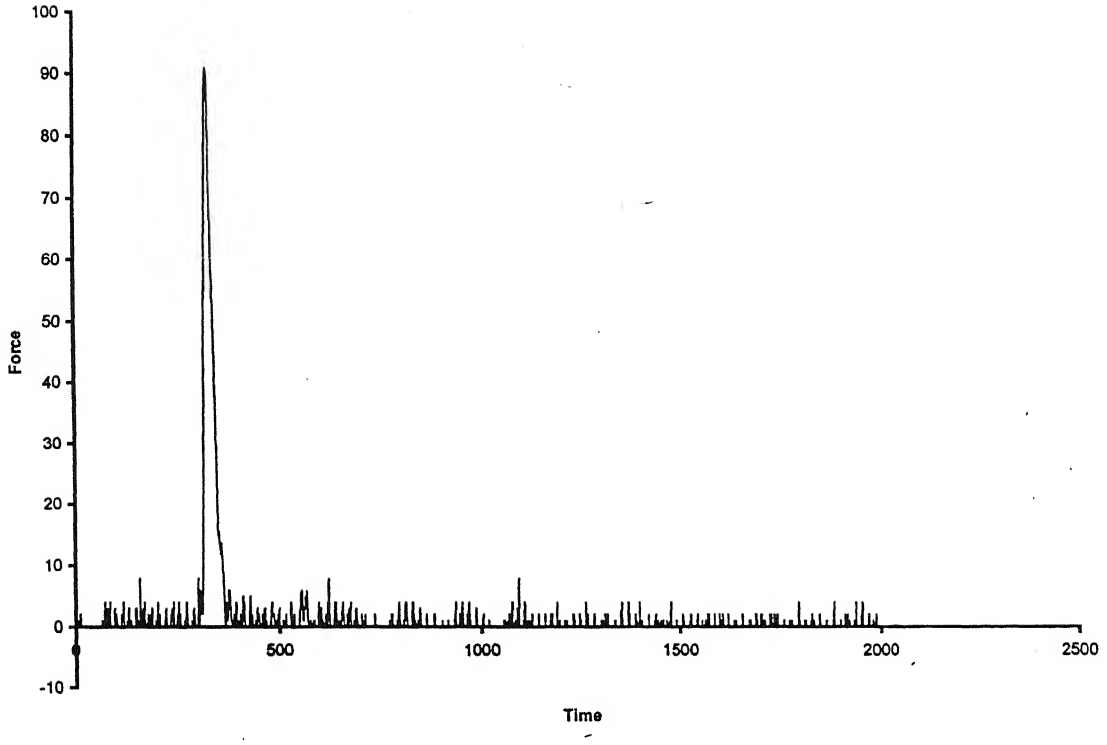

Fig 3.21 Graph of Force and Time during drop weight impact testing for PMMA sheets with polymer.

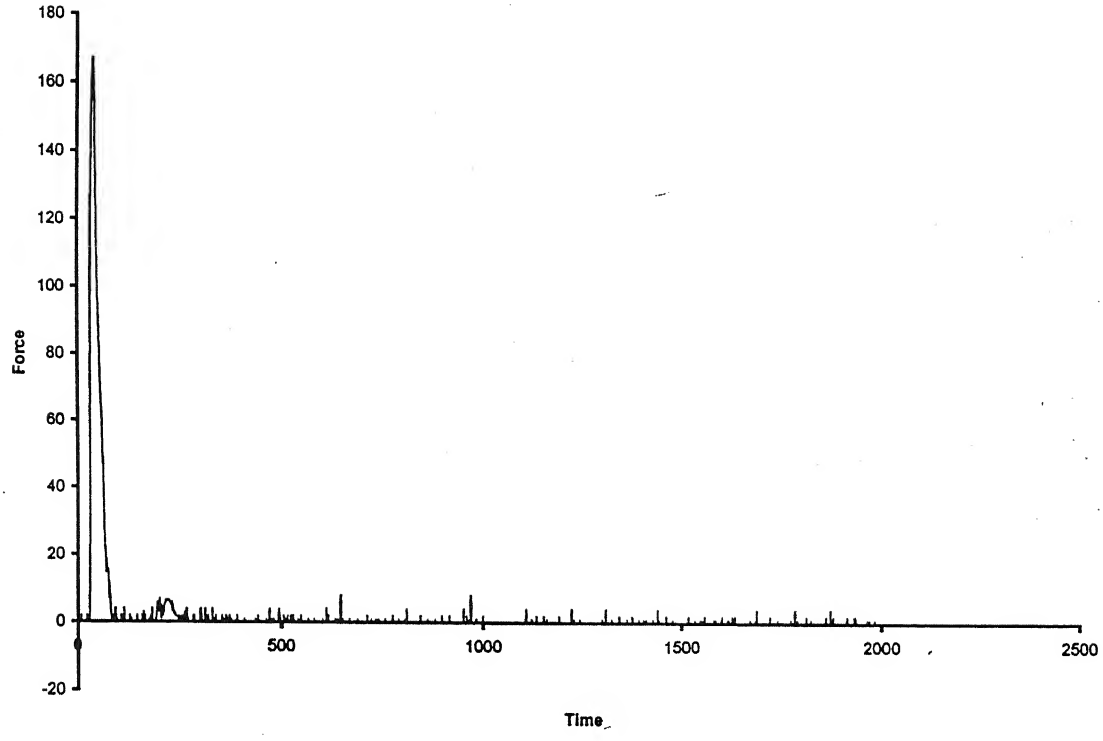

Fig 3.22 Graph of Force and Time during drop weight impact testing for PMMA sheets with polymer syrup containing 2% non settling nano particles.

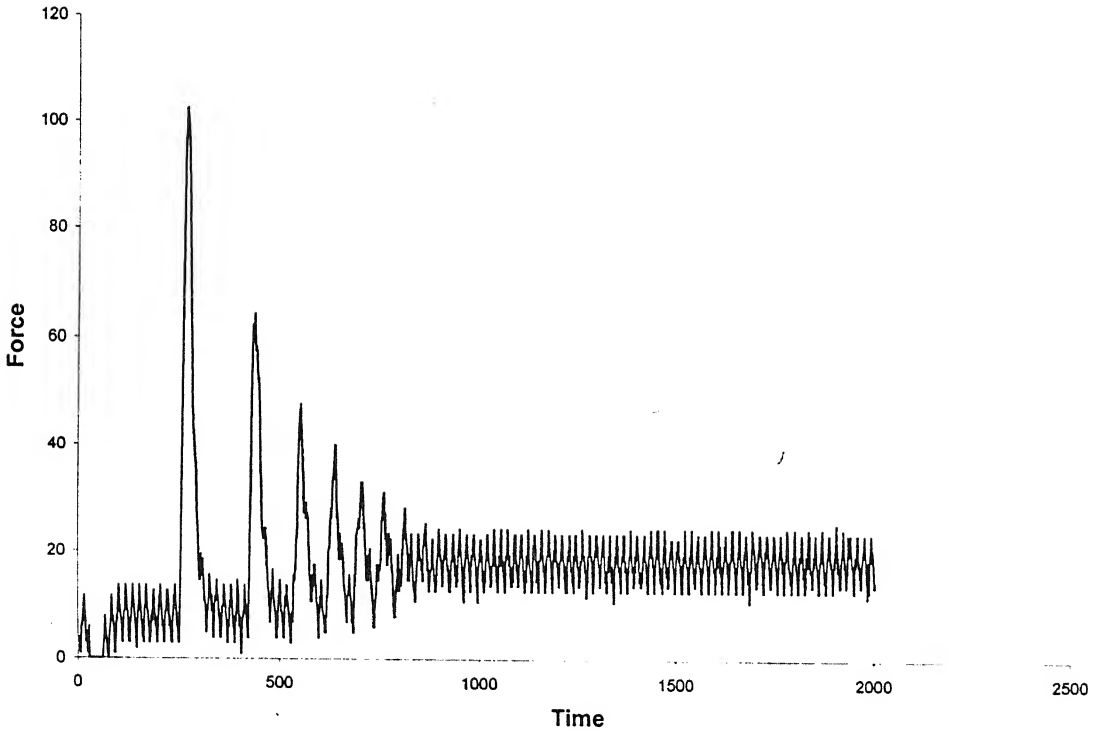

Fig 3.23 Graph of Force and Time during drop weight impact testing for empty Poly Carbonate sheets.

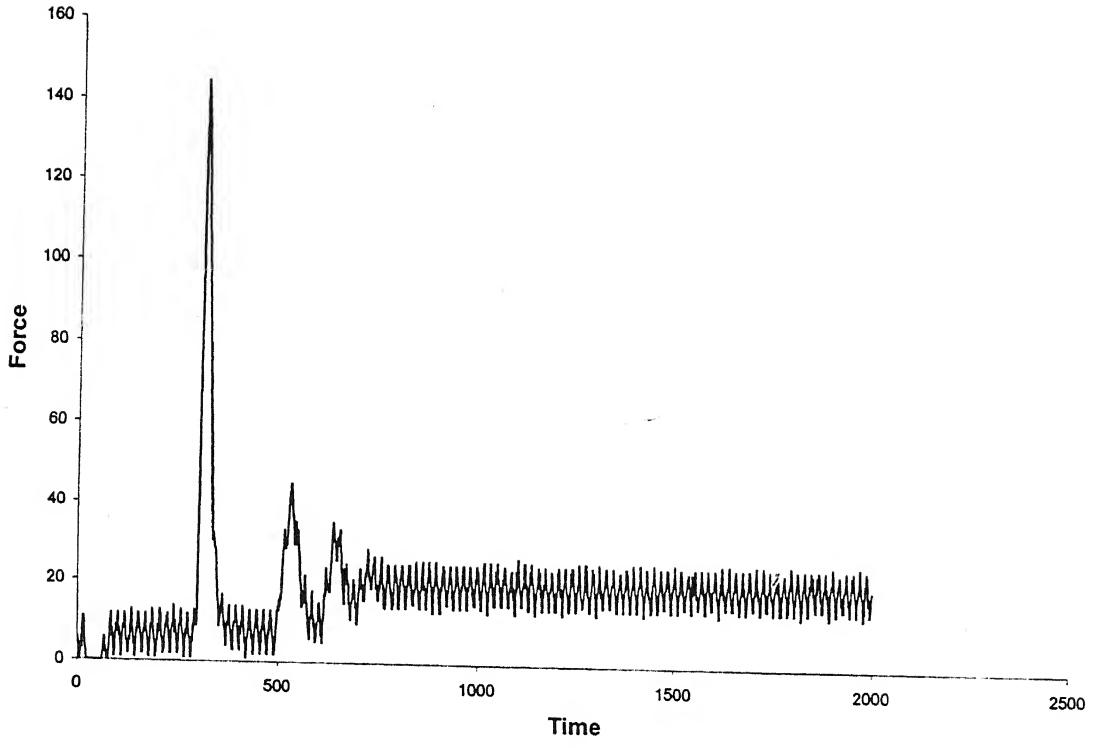

Fig 3.24 Graph of Force and Time during drop weight impact testing for Poly Carbonate sheets with polymer.

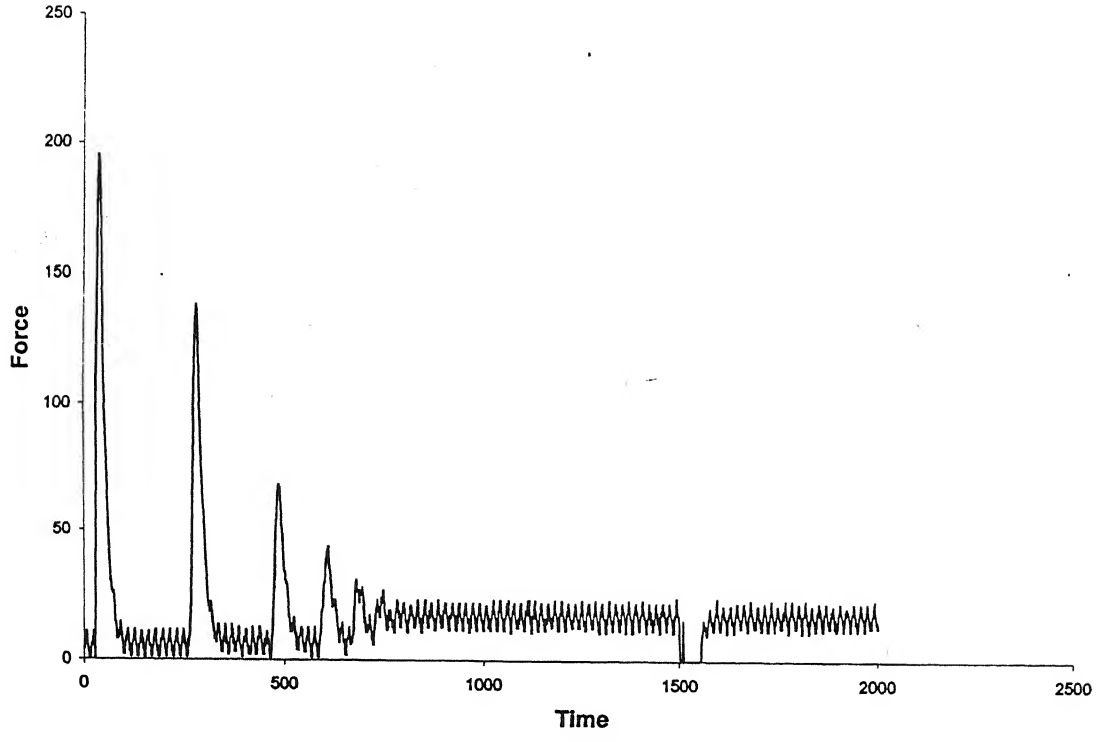

Fig 3.25 Graph of Force and Time during drop weight impact testing for Poly Carbonate sheets with polymer syrup containing 2% non settling nano particles.

Chapter 4

CONCLUSIONS

Alumina nano particles having grain size 28 nm were successfully prepared by auto ignition of aluminum nitrate (10.5 g) and urea (2.8 g). These particles were modified with methacrylol isocyanate, synthesized by the reaction of methacrylol chloride and sodium azide. The XRD analysis showed that the modified nano particles have similar crystal structure with the average grain size in the range of 38 nm. The TEM analysis showed the particle size of nano alumina in the range of 35 nm, this was confirming the estimation based on XRD. TGA of nano alumina showed that there was only 10 % weight loss for nano alumina upto 900^0C, whereas there was 23% weight loss for the modified nano alumina upto 900^0C.

Polymer syrup containing non settling nano particles were prepared using 2% modified nano alumina and MMA polymerized by dual initiating system containing Benzoylperoxide (BPO), Azobisisobutyronitrile (AIBN) and Dimethylaniline (DMA) accelerator. This polymer syrup was applied in between PMMA sheets and Polycarbonate sheets using an air spray. These composite sheets were tested by Bullet Firing Machine and Vertical Drop Weight Impact Testing Machine. The results of Bullet Firing Machine when fired with a bullet speed of 62 m/s indicated that empty PMMA sheets were completely damaged and PMMA sheets with polymer syrup showed 59% damage while PMMA sheets with polymer syrup containing non settling nano particles has only 9% damaged area. As opposed to this, polycarbonate sheets when fired with a bullet speed of 91 m/s indicated that Polycarbonate sheets with polymer has 34% damaged area; whereas

Polycarbonate sheets with syrup containing non settling nano particles has shown no damage.

The results of Drop Weight Impact Testing Machine showed that, for empty PMMA sheets the maximum load was 55 Kg, for PMMA sheets with polymer has a maximum load of 90 Kg and for PMMA sheets with polymer syrup containing non settling nano particles has a maximum load of 166 Kg. As opposed to this, for empty Polycarbonate sheets the maximum load was 102 Kg, for Polycarbonate sheets with polymer has maximum load of 144 Kg and for Polycarbonate sheets with polymer syrup containing non settling nano particles has a maximum load of 193 Kg.

8) J. H. Chang, Y. U. An, Nano composites of polyurethane with various organoclays: Thermo mechanical properties, morphology and gas permeability: J.Polym. Phys. 40 (2002) 670-677.

9) S.A. Zavyalov, A.N. Pivkina, J.Schoonman, Formation and characterization of metal-polymer Nano structured composites: Solid State Ionics 147 (2002) 415-419.

10) K. Niihara, New design concept of structural ceramics: Ceramic nano composites, Journal of the ceramic society: Japan 99(10) (1991) 974.

11) Sumita M, Shizuma T, Miyasaka K, Ishikawa K. J Macromol Sci Phys 1983; B 22: 601.

12) Brian L.Cushing, Vladimir L.Koleshnichenko, Charles J. O'Connor, Recent Advances in the liquid-phase synthesis of inorganic nano particles: Chem., Rev. 104 (2004) 3893-3946.

13) Ring, T.A. Fundamentals of Ceramic Powder Processing and Synthesis, Academic Press: San Diego, CA, 1996.

14) Dirksen, J.A.; Ring, T.A., Fundamentals of crystallization: kinetic effects on particle size distributions and morphology: Chem. Eng. Sci. 46 (1991) 2389-2427.

15) Karpinski, P. H.; Wey, J.S. In Handbook of Industrial Crystallization, 2nd edition; Myerson, A.S., Ed.; Butterworth-Heinemann: Stoneham, MA (2001).

16) Tromp, R.M.; Hannon, J. B., Thermodynamics of nucleation and growth: Surface Rev. Lett. 9 (2002) 1565-1593.

17) Blackadder, D.A., Chem. Eng. (1964) CE 303.

18) J. Su, Q. L. Zhang, C. J. Gu, D. L. Sun, Z. B. Wang, H. L. Qiu, A. H. Wang, S. T. Yin, Preparation and characterization of $Y_3Al_5O_{12}$(YAG) nano powder by Coprecipitaion method: Materials Research Bulletin (2005) In Press.

19) Dong-Hwang Chen and Yuh-Yuh Chen, Synthesis of strontium ferrite nanoparticles by coprecipitation in the presence of polyacrylic acid: Materials research Bulletin 37 (2002) 801-810.

20) Brinker, C. J.; Scherer, G. W. Sol-Gel Science: The physics and chemistry of sol-gel processing; Academic Press: San Diego, CA, 1990.

21) Wright, J. D.; Sommerdijk, N. A. J. M. Sol-gel Materials: Chemistry and applications, Taylor and Francis: London, 2001.

22) Pierre, A. C. Introduction to sol-gel processing: Kluwer: Boston, 1998.

23) Yan, C.; Sun, L.; Cheng, F. Handbook of nanophase and nanostructured materials; 2003; p72.

24) Cheng-min Shen, Xiao-gang Zhang, Ying-ke Zhou, Hu-lin Li; Preparation and characterization of nanocrystalline $Li_4Ti_5O_{12}$ by sol-gel method: Materials Chemistry and Physics 78 (2002) 437-441.

25) Jun Wang, Jian Sha, Qing Yang, Youwen Wang and Deren Yang, Synthesis of aluminium borate nanowires by sol–gel method: Materials Research Bulletin In press (2005).

26) Liqun Mao, Qinglin Li, Hongxin Dang and Zhijun Zhang, Synthesis of nanocrystalline TiO_2 with high photoactivity and large specific surface area by sol–gel method: Materials Research Bulletin 40 (2005) 201-208.

27) Rajamathi, M.; Seshadri, R. Curr. Opin., Oxide and chalcogenide nanoparticles from hydrothermal/solvothermal reactions: Solid State Mater. Sci. 2 (2002) 337-345.

28) Cansell, F.; Chevalier, B.; Demourgues, A.; Etourneau, J.; Even, C.; Garrabos, Y.; Pessey, V.; Petit, S.; Tressaud, A.; Weill, F. J., Supercrtical fluid processing: a new route for materials synthesis: Mater. Chem. 9 (1999) 67-75.

29) Cheng, H.; Ma, J.; Zhao, Z.; Qi, L., Hydrothermal Preparation of Uniform Nanosize Rutile and Anatase Particles: Chem. Mater. 7 (1995) 663-671.

30) Jian Yang, Guang-Hui Cheng, Jing-Hui Zeng, Shu-Hong Yu, Xian-Ming Liu and Yi-Tai Qian, Shape control and characterization of transition metal diselenides MSe_2 (M= Ni, Co, Fe) prepared by a solvothermal-reduction process: Chem. Mater. 13 (2001) 848-853.

30) P.Kumar and K.L.Mittal,Handbook of microemulsion science and technology, Marcel Dekker, New York, 1999 Part III, 452-742; J.Texter, Reactions and synthesis in surfactant systems, Surfactant Science Series, Vol.100, Marcel Dekker, 2001 Part IV, 577-665

32) Langevin, D. In Structure and Reactivity in Reverse Micelles; Pileni, M.P., Ed.; Elsevier: Amsterdam, 1989.

33) A. M. North, The Collision theory of chemical reactions in liquids (Methuen, London, 1964).

34) Winsor, P. A, Binary and multicomponent solutions of amphiphilic compounds. Solubilization and the formation, structure, and theoretical significance of liquid crystalline solutions: Chem. Rev. 68 (1968) 1-40.

35) T. F. Towey, A. N. Khan-Lodhi, and B. H. Robinson, Kinetics and mechanism of formation of quantum sized cadmium sulphide particles in water-aerosol-OT-microemulsions: J. Chem. Soc., Faraday Trans. 86 (1990) 3757-3762.

36) A. Agostiano, M. Catalano, M. L. Curri, M. Della Monica, L. Manna, L. Vaasanelli, Synthesis and structural characterization of CdS nanoparticles prepared in a four-components "water-in-oil" microemulsion: Micron 31 (2000) 253-258.

37) G. R. Karagedov and N. Z. Lyakhov, Preparation and sintering of nanosized α-Al_2O_3 powder: NanoStructured Materials 11 (1999) 559-572.

38) E. G. Avvakurnov, Methods of mechanical activation of chemical processes, Nauka, Novosibirsk (1986).

39) H. L. Wen, Y. Y. Chen, F. S. Yen, C. Y. Huang, Size characterization of γ- and α-Al_2O_3 crystallites during phase transformation, Nano Structured Materials 11 (1999) 89-101.

40) A. Kumar, R. K. Gupta, Fundamentals of Polymers, 1^{st+} edition, McGraw-Hill, Newyork, 1998

41) P. H. T. Vollenberg, D. Heikens, Particle size dependence of the young's modulus of filled polymers: 1.preliminary experiments: Polymer 30 (1989) 1656-1662.

42) C. –M. Chan, J. Wu, J. –X. Li, Y. –K. Cheung, Polypropylene/calcium carbonate nano composites: Polymer 43 (2002) 2981-2992.

43) Z. S. Petrovic, I. Javni, A. Waddon, G. Banhegyi, Structure and properties of polyurethane-silica nano composites: J. Appl. Polym. Sci. 76 (2000) 13-151.

44) M. Z. Rong, M. Q. Zhang, Y. X. Zheng, H. M. Zeng, R. Walter, K. Friedrich, Structure-property relationships of irradiation grafted nano-inorganic particle filled polypropylene composites: Polymer 42 (2001) 167-183.

45) F. Yang, Y. Ou, Z. Yu, Polyamide 6/silica nano composites prepared by insitu polymerization: J.Appl. Poly. Sci. 69 (1998) 355-361.

46) T. Ou, F. Yang, Z.-Z. Yu, A new conception on the toughness of nylon 6/silica nano composite prepared via insitu polymerization: J. Polym. Sci. B: Polym. Phys. 36 (1998) 789-795.

47) E. Reynaud, T.Jouen, C. Gautheir, G. Vigier, Synthesis and thermal characterization of crystallizable poly(caprolactone)/poly(hexamethylene terephthalate) block copolymer: Polymer 42 (2001) 8759-8768.

48) J.-X. Li, J. Wu, C. M. Chan, Thermoplastic nano composites: Polymer 41 (2000) 6935-6937.

49) A. Okada, T. Usuki, O.Kurauchi, Kamigaito, in: J. E. Mark, C. Y.-C. Lee, P. A. Branconi (Eds.), ACS Symposium, 1995, pp. 55-65.

50) Y. T. Vu, J. E. mark, L. H. Pham, M. Engelhardt, Clay nanolayer reinforcement of cis-1,4-polyisoprene and epoxidized natural rubber: J.Appl. Poly. Sci. 82 (2001) 1392-1403.

51) Yi- quan Wu, Yu-feng Zhang, Xiao-xian Huang, Jing-kun Guo, Preparation of plate like nano alpha alumina particles: Ceramics Internations 27 (2001) 265-268.

52) S. Bhaduri, E. Zhou and S. B. Bhaduri, Auto ignition processing of nanocrystalline <-Al_2O_3: Nanostructured Materials 7 (1996) 487-496.

53) S. R. Jain, K. C. Adiga, V. R. Pai Verneker, A new approach to thermochemical calculations of condensed fuel-oxidizer mixtures: Combustion and Flame 40 (1981) 71-79.

54) Weast, R. C. (Ed.), Handbook of chemistry and physics, Chemical Rubber, Cleveland, 1969, pp. D-184-D189.

55) I. L . Finar, Organic Chemistry Volume 1: The Fundamental Principles, sixth edition, published by ELDS, 1989, p 256.

56) I. L . Finar, Organic Chemistry Volume 1: The Fundamental Principles, sixth edition, published by ELDS, 1989, p 265.

57) G. Pugazhenthi, Anil Kumar, Enzyme membrane reactor for hydrolysis of olive oil using lipase immobilized on modified PMMA composite membrane: Journal of Membrane Science, 228 (2004) 187-197.

58) Powder Diffraction file (1985) vol.10 p173, Published by International centre for diffraction data.

59) C. Suryanarayana, M. Grant Norton, X-Ray Diffraction, A Practical Approach: Plenum Press, 1998, p 207.

60) http://wwwchem.csustan.edu/Tutorials/INFRARED.HTM